A Y-linked duplication of anti-Mullerian hormone is the sex determination gene in threespine stickleback

Matthew J. Treaster, Jenny McCann, Kyra S. Solovei, Ryan J. Palmieri, and Michael A. White

Department of Genetics, University of Georgia, Athens, GA 30602

Corresponding Author:
Michael A. White
Department of Genetics, University of Georgia
120 E Green St
Athens, GA 30602
Whitem@uga.edu

Abstract

Many taxa have independently evolved genetic sex determination where a single gene located on a sex chromosome controls gonadal differentiation. The gene anti-Mullerian hormone (*amh*) has convergently evolved as a sex determination gene in numerous vertebrate species, but how this gene has repeatedly evolved this novel function is not well understood. In the threespine stickleback (*Gasterosteus aculeatus*), *amh* was duplicated onto the Y chromosome (*amhy*) ~22 million years ago. To determine whether *amhy* is the primary sex determination gene, we used CRISPR/Cas9 and transgenesis to show that *amhy* is necessary and sufficient for male sex determination, consistent with the function of a primary sex determination gene. While we find substantial regulatory evolution has occurred in *amhy*, we did not observe an increase in *amhy* expression across early development relative to its autosomal paralog, *amha* or a significant difference in total *amh* dosage between males and females around the time of sex determination. This indicates the mechanism of sex determination may involve subtle changes in cell-specific expression or coding sequence evolution. The creation of sex reversed lines also allowed us to investigate the genetic basis of secondary sex characteristics. Threespine stickleback have striking differences in behavior and morphology between sexes. Here we show one of the classic traits important for reproductive success, blue male nuptial coloration, is controlled by both Y-linked genetic factors as well as hormonal factors independent of sex chromosome genotype. This research establishes stickleback as a model to investigate how *amh* regulates gonadal development and how this gene repeatedly evolves novel function in sex determination. Analogous to the “four core genotypes” model in house mice, sex-reversed threespine stickleback offer a new vertebrate model for investigating the separate contributions of gonadal sex and sex chromosomes to sexual dimorphism.

Introduction

For species that have two discrete sexes, sex determination is the process that designates whether an individual will become male or female [1,2]. While this process is essential to the fitness and survival of a species, it is regulated by a surprising variety of initial cues and can incorporate a range of extrinsic signals as well as intrinsic genetic factors often located on sex chromosomes [1–3]. Numerous eukaryotic taxa have convergently evolved sex chromosomes, such as the XX-XY system found in mammals, to regulate this critical developmental process [1,2]. Sex chromosomes are derived from a pair of autosomes after one of these autosomes acquires a sex determining (SD) gene [4]. Suppression of recombination around this gene leads to sequence divergence of the two autosomes into a pair of divergent sex chromosomes [4]. Why this recombination suppression occurs is not clear; however, the prevailing model is that suppressed recombination will be selected for to link an SD gene with nearby sexually antagonistic mutations that are beneficial to one sex but detrimental to the other [4–6]. One remarkable observation that has emerged from comparative studies is the SD gene responsible for initiating development of testes or ovaries in their respective sex is incredibly variable [1,7]. How the otherwise well conserved sex differentiation developmental network can be regulated by such a diverse range of SD genes remains poorly understood.

A wide variety of genes have evolved novel function as sex determination genes, but some genes appear predisposed to acquiring this role and have convergently evolved as sex determination genes in distantly related taxa [7]. *Sox3*, the ancestor of the mammalian SD gene *Sry,* also acts as the SD gene in the Indian rice fish (*Oryzias dancena*) [8]. SD genes derived from *dmrt1* are found in birds [9], the African clawed frog (*Xenopus laevis*) [10], and medaka (*Oryzias latipes*) [11,12]. The most prevalent SD gene among vertebrates by far is *anti-Mullerian hormone* (*amh*) [7]. Independently acquired Y-linked copies of *amh* or its dedicated receptor, *amhrII*, have been identified in at least twelve different clades of teleost fish [13–24] as well as in monotremes [25]. These Y-linked copies of *amh* and *amhrII* are presumed to be SD genes in all of these taxa. Although *amh* accounts for over one quarter of identified SD genes in

vertebrates, how *amh* controls this critical developmental process and evolves novel function in sex determination is not clear [7].

Amh is a member of the transforming growth factor beta (TGF-β) family of proteins that are shared across vertebrates (Reviewed in [26,27]). *Amh* is unique among TGF-β hormones as it has only one identified type II receptor, *amhrII*, of which *amh* is the only known ligand [28–30]. *Amh* and its receptor were first identified for their role in reproductive tract development in mammals, where secretion of Amh by the developing testes causes regression of the primordial female reproductive tract, the Müllerian ducts [31]. Disruption of *amh* signaling in teleosts, which lack Müllerian ducts, causes over proliferation of germ cells in the gonad and can interfere with sex determination, even in species were *amh* is not the SD gene [32–34]. This suggests the ancestral function of *amh* is likely in germ cell proliferation and maintenance which, if disrupted, can disrupt sex determination, but how this disruption occurs is not clear. It also is not known whether Y-linked copies of *amh* that have convergently evolved function in sex determination control the downstream network in the same way or if *amh* can regulate sex differentiation through a variety of distinct mechanisms.

Species of stickleback fish (family Gasterosteidae) have multiple, independently evolved sex chromosome systems, making them an ideal model for investigating the origins of sex chromosomes and SD genes [20,35–38]. Two separate duplications of *amh* that are associated with male sex have been identified within stickleback fish. In the genus *Gasterosteus*, *amh* was duplicated from autosome 8 onto autosome 19 approximately 22 million years ago (Mya), leading to the evolution of a Y chromosome [20,39]. An independent duplication of *amh* onto chromosome 20 was identified in the brook stickleback, *Culea inconstans*. This duplication differs from the ancestral copy on autosome 8 by only a handful of single nucleotide polymorphisms (SNPs), suggesting this duplication occurred much more recently than in the genus *Gasterosteus* [22,40]. Consistent with its recent acquisition, the duplicate copy of *amh* is not a fully penetrant SD gene, and its association with male sex varies across populations [40].

This provides a unique opportunity to examine the convergence evolution of *amh* as an SD gene at two dramatically different stages of sex chromosome evolution.

The threespine stickleback (*Gasterosteus aculeatus*) is a powerful emerging model for evolutionary and developmental biology with a robust set of genomic and functional genetic tools [41,42]. Their small size, large clutch sizes, and relatively short generation time make them a highly tractable model for studying the developmental mechanisms of *amh* as an SD gene. Threespine stickleback also have many well-studied sexually dimorphic traits and mating behaviors that have provided substantial insight into the evolution of sexual dimorphism and its effect on fitness [43–64]. Like other members of its genus, threespine stickleback have retained a functional copy of autosomal *amh* on chromosome 8 (hereafter called *amha*) as well as the Y-linked *amhy*. The AMH prodomain and TGF-β signaling domain within *amhy* are conserved (Fig S1), indicating the Y-linked duplicate is likely functional [20]. In addition, *amhy* is expressed in larvae around the time of sex determination, consistent with a role in initiating male development [20]. Beyond this, it is unknown whether *amhy* has a functional role in male sex determination. In this study, we show that *amhy* is both necessary and sufficient for male sex determination in the threespine stickleback, demonstrating that it is the SD gene in this species. We also perform RNA-seq of stickleback embryos and larvae to characterize expression of *amhy* and early transcriptional differentiation of males and females. Our findings establish stickleback fish as a premier model to study both the molecular mechanisms of *amh* based sex determination as well as the convergent evolution of *amh* as a sex determination gene in vertebrates.

Results

CRISPR/Cas9 knockout of *amhy* caused male-to-female sex reversal in XY fish.

If *amhy* is the SD gene in threespine stickleback, it should be both necessary and sufficient for male sex determination. To test this, we first knocked out function of *amhy* in XY

118 fish using CRISPR/Cas9. We designed two sgRNAs targeting exon 1 and exon 3 of *amhy* (Fig
119 1). We injected stickleback embryos from lab-reared fish derived from two independent marine
120 populations (Port Gardner Bay and Japan Pacific Ocean) with CRISPR ribonucleoprotein (RNP)
121 made with one of the two sgRNAs. 8/17 (47%) of F0 XY fish injected with RNP exhibited male-
122 to-female sex reversal. For all eight XY sex reversed fish, we observed ovaries with all cell
123 types seen in wildtype ovaries (Fig S2).

124 F0 crispants are often mosaic for mutations induced by CRISPR/Cas9 gene editing,
125 which can cause variation in observed phenotypes. To generate non-mosaic F1 gene-edited
126 fish, we used two F0 XY males that had heritable germline mutations in *amhy* but were not sex
127 reversed, indicating they likely did not have *amhy* mutations in cell-lineages important for sex
128 determination. Sperm from these fish were used to fertilize eggs from wildtype XX females. F1
129 offspring from these crosses inherited frameshift mutations in *amhy*, identified by Sanger
130 sequencing (Fig S3). We analyzed five F1 males from one F0 crispant with mutations in exon 1
131 and 21 F1 males from one F0 crispant with mutations in exon 3. All 26 F1 fish exhibited
132 complete male-to-female sex reversal and developed ovaries morphologically and histologically
133 indistinguishable from wildtype XX females (Fig 1C). No F1 XY fish showed development of
134 testis or ambiguous gonad tissue with any visible spermatocyte production. We identified three
135 loss of function alleles in exon 1 of *amhy* (Fig 1A) and one in exon 3 (Fig 1B). In ten F1 fish, the
136 region of *amhy* in exon 3 targeted by CRISPR/Cas9 could not be amplified. PCR of exons 1 and
137 7 showed the presence of these distal portions *amhy*, but PCRs spanning a large putative
138 deletion all failed to amplify, suggesting a chromosomal rearrangement disrupted *amhy* in these
139 fish. As a specific mutation could not be positively identified, these samples were excluded from
140 further analysis and final counts.

141 We analyzed the expression of canonical male differentiation genes *amha* and *dmrt1*
142 and female differentiation genes *foxl2* and *cyp19a1a* using *in situ* hybridization on wildtype and
143 F1 XY *amhy*-KO ovaries (Fig 2, Fig S4). We also analyzed *gsdf* as a positive control, as this

144 gene is expected to be expressed in somatic gonadal cells of both sexes [65]. Both wildtype and
145 sex reversed ovaries showed expression of *foxl2* and *cyp19a1a* in somatic cells. Expression of
146 *amha* and *dmrt1* was minimal and restricted to oocytes when present as has been observed in
147 some species of fish [21,66–69]

148 Knockout of *amh* or *amhrII* in teleost species without amh-based sex determination has
149 caused male-to-female sex reversal, including in lab strains of zebrafish which lack sex
150 chromosomes (reviewed in [70]) and medaka which have an XX-XY system with a *dmrt1*
151 derived sex determination gene [32]. Thus, it is possible that off-target mutations of the
152 homologous *amha* could contribute to the sex reversal observed in F1 *amhy* mutants. Both
153 sgRNAs have multiple mismatches to their homologous region in *amha*, and we verified that all
154 F1 XY *amhy*-KO females did not have mutations within *amha* by sanger sequencing (Fig S5).
155 This demonstrates that the sex reversal phenotype was not caused by mutations of *amha*. We
156 also investigated whether the sex reversal phenotype was caused by a mutation at an unknown
157 autosomal locus. Such an autosomal mutation must be dominant since we observed male-to-
158 female sex reversal in heterozygous XY F1 fish. F1 XX siblings of sex reversed XY fish would
159 also be heterozygous for this mutation, and half of their F2 XY progeny would be sex reversed.
160 We crossed two F1 XX PG females with wildtype XY males and phenotyped F2 offspring for sex
161 reversal. All 16 F2 XY fish were phenotypically male, indicating that sex reversal in F1 XY *amhy*-
162 KO fish was not caused by an off-target autosomal mutation.

163

164 **Introduction of an *amhy* transgene caused female-to-male sex reversal in XX fish.**

165 To determine if *amhy* is sufficient for male sex determination, we created a construct
166 (pT2-5amhy2.5,Xla.Ef1a:EGFP) containing an 11 kb region of the Y chromosome which
167 includes *amhy*, 5 kb of upstream sequence, and 2.5 kb of downstream sequence (Fig S6F). By
168 including the surrounding non-coding sequences, we aimed to recapitulate the endogenous
169 expression patterns of *amhy.* An Xla.Ef1a:EGFP cassette downstream of *amhy* was included to

170 facilitate the screening of injected embryos for transgene integration. These components were
171 flanked by *Tol2* transposon sequences to facilitate random integration into the genome by the
172 Tol2 transposase [71,72]. 16 F0 XX fish showed positive GFP expression and successful
173 transgene integration, detected through PCR genotyping (Fig 3D). At reproductive age, all 16 F0
174 XX *Tg(amhy,EGFP)* were female-to-male sex reversed, developing testes rather than ovaries
175 (Fig 3A). All 10 control F0 XX fish injected with the control Xla.ef1a:EGFP transgene showed
176 positive presence of the transgene, but did not show any signs of sex reversal and developed
177 cytologically normal ovaries (Fig 3B). We also analyzed the expression of *amha, dmrt1, foxl2*,
178 *cyp19a1a,* and *gsdf* using *in situ* hybridization on wildtype and F0 XX *Tg(amhy,EGFP)* testes
179 (Fig 2, Fig S7). Both wildtype and sex reversed testes showed strong expression of *amha* and
180 *dmrt1* in somatic cells and no discernable expression of *foxl2* or *cyp19a1a*.
181 We attempted to constitutively express *amhy* using a synthetic exon-only coding
182 sequence with an N-terminus FLAG tag joined to a 3' EGFP by a P2A self-cleaving peptide
183 [73,74]. Plasmids were made using the *D. rerio* ubiquitin promoter [75] or the *X. laevis* ef1a
184 promoter [76] to drive expression of the amhy,EGFP construct (Fig S6). Transgenes with the
185 respective promoter driving expression of only EGFP were used as controls. Somatic EGFP
186 expression was observed with both control transgenes indicating these promoters can drive
187 expression in stickleback. Neither the Dre.Ubi:amhy,EGFP nor the Xla.Ef1a:amhy,EGFP
188 transgene produced any larvae with visible EGFP expression, indicating that the *amhy*
189 transgenes were failing to integrate or be actively expressed in any embryos. We hypothesize
190 that the failure to constitutively express *amhy* may be due to cytotoxicity of extremely high and
191 widespread expression of *amh* using these non-native, constitutive promoters.
192
193 **Sex reversed *amhy* mutants produce viable gametes but are subfertile.**
194 Sex-reversed XY *amhy*-KO females produced mature oocytes and became gravid, but
195 they were subfertile compared to wildtype females. To assess fertility, we crossed three F1 XY

196 *amhy*-KO females to wildtype XY males. These clutches all showed extremely low viability rates,
197 between 2% and 6% (Table S1), measured by presence of a gastrula and active epiboly 12 to
198 24 hours after fertilization (haf). One of the three F1 fish was crossed four additional times and
199 showed improvement in viability with the subsequent crosses. The viability rates of the fourth
200 and fifth cross were 78% and 79% respectively, producing a total of 148 viable F2 eggs (Table
201 S1). Three days after fertilization, 50 of the 148 eggs had arrested development. We were able
202 to genotype 48 of the failed embryos. Three-quarters of these (36) carried no X chromosome
203 and both the paternally transmitted Y chromosome (Y^p) and the maternally transmitted *amhy*-
204 KO Y chromosome (Y^m) (Fig 4). The remaining embryos were reared to adulthood and 92 were
205 genotyped for their sex chromosome complement. No adult YY fish were observed, indicating
206 that the YY genotype is embryonic lethal due to the missing X chromosome. XY^m females were
207 found to transmit the X and Y^m chromosome with equal frequency, indicating there was not any
208 biased transmission of the X or Y chromosome during female meiosis (36 Y^pY^m embryos out of
209 148 total does not deviate from a 1:3 Mendelian ratio; chi-squared = 0.0360; p = 0.8494; of the
210 92 adult F2s genotyped 36 XX, 27 XY^p , and 29 XY^m does not deviate from the expected 1:1:1
211 ratio; chi-squared = 1.457; p = 0.4827). Subfertility also extended to second generation sex-
212 reversed XY females. We crossed 11 F2 females with wildtype XY males. The clutch size did
213 not differ significantly between XY^m and XX females (Fig 4C; Table S2). However, the viability
214 rate was substantially lower in the F2 XY^m females, similar to the F1 generation (Fig 4D, Table
215 S2). Two XY^m F2 females were also eggbound and were unable to be stripped of eggs.
216 Female-to-male sex reversed F0 XX fish had varied fertility. Four of the 16 XX
217 *Tg(amhy,EGFP)* males had testes morphologically resembling those of a fertile, wildtype male.
218 12 XX males had abnormally small and underdeveloped testes and four. We performed crosses
219 with all four males with mature testes with wildtype XX females. One male was extremely
220 subfertile (27 viable of 911 eggs). The remaining three males showed normal viability rates (78
221 viable of 97 total eggs, 84 viable of 89 total eggs, and 231 viable of 235 total eggs). One fertile

222 male also produced offspring with somatic GFP expression at a very low frequency (16/231)
223 indicating a heritable germline integration of the transgene had occurred. Histology of these
224 males showed key differences between fertile, subfertile, and hypotrophic testes (Fig 3A).
225 Fertile males had normal testis histology with visible mature spermatozoa. The subfertile male
226 testis lacked spermatozoa, instead containing immature spermatocytes and round spermatids
227 concordant with its reduced fertility. Histology of the hypotrophic testes were abnormal and did
228 not show any clearly identifiable germ cells. This phenotypic variation may be a result of
229 variable *amhy* expression influenced by transgene copy number and insertion location.
230

231 **Male nuptial coloration is present in both sex reversed genotypes**

232 Male nuptial coloration is one of the most prominent sexually dimorphic characteristics in
233 threespine stickleback. During their breeding season, males from many stickleback populations
234 develop throats and dark blue eyes and bodies [77]. To investigate the separate contributions of
235 gonadal and genotypic sex on this trait, we compared coloration in mature sex reversed XY
236 *amhy*-KO females and XX *Tg(amhy,EGFP)* males to wildtype XX and XY fish (Fig 5). Nuptial
237 coloration is prominent in XY males once reproductively mature. Neither *amhy* mutant genotype
238 fully recapitulates wildtype XY male coloration, but both XX males and XY females show
239 elements of male nuptial coloration and are distinct from wildtype XX females. In XX males,
240 nuptial coloration was present in all three fertile males, but not in the male with immature sperm
241 or any males with hypotrophic testes. Together, these findings show that male nuptial coloration
242 is influenced both by hormones produced by the testis and by sex chromosome genotype, but
243 both male gonad differentiation and an XY genotype is needed to present full male nuptial
244 coloration.
245

246 ***amhy* does not have distinct expression timing relative to *amha***

247 Since Amh shows high specificity for its dedicated receptor, AmhrII, [28–30] we predicted
248 that *amhy* would be functionally constrained regarding coding sequence evolution and would
249 instead evolve novel function through regulatory changes. We investigated the degree of
250 sequence conservation within putative regulatory regions (2 kb upstream and downstream of
251 the coding sequence), of *amhy* relative to *amha*. We also compared sequence similarity
252 between *amha* and the autosomal *amh* in the ninespine stickleback (*Pungitius pungitius*). The
253 divergence time between threespine and ninespine stickleback is approximately 26 Mya [78],
254 similar to the 22 Mya divergence time between the threespine *amha* and *amhy* [20]. There was
255 less sequence identity between the coding sequences of threespine *amha* and *amhy* than
256 between threespine *amha* and ninespine *amh* (Fig 6, Table 1). This is consistent with weaker
257 purifying selection acting on the Y chromosome due to a lack of recombination [79]. This was
258 also supported by a higher dN/dS value between threespine *amha* and *amhy* than between
259 threespine *amha* and ninespine *amh*. Alternatively, this could be due to positive selection acting
260 on coding sequence changes to *amhy*. The sequence identity of upstream and downstream
261 regions was much lower between *amha* and *amhy* than between *amha* and ninespine *amh*,
262 indicating *amhy* has undergone significant regulatory evolution since its duplication onto the Y
263 chromosome, which may cause differences between *amha* and *amhy* expression.
264 To determine whether expression of these genes differ throughout development, we
265 sequenced the total transcriptomes from prehatching embryonic stages 17 (early
266 somitogenesis, ~43 haf), 20 (onset of pigmentation, ~73 haf), and 23 (completion of yolk sac
267 circulation, ~122 haf) as well as larvae 0, 4, and 8 days after hatching (dah), where hatching
268 occurred around 200 haf [80]. The earliest identified morphological difference between male and
269 female threespine stickleback is a difference in primordial germ cell count at 3 to 4 dah [81]. Sex
270 determination should begin sometime prior to this stage. We predicted that the unique
271 regulatory architecture of *amhy* resulted in earlier expression timing relative to *amha.* Thus,
272 *amhy* would be expressed at higher levels relative to *amha* early in development in order to

initiate sex determination. As the gonad differentiates, *amha* expression should increase relative to *amhy* due to the canonical role of *amh* in male differentiation. This pattern has been observed in Japanese flounder [15] and Patagonian pejerrey [13] which also have *amhy* SD genes. Contrary to our prediction, we found that *amhy* expression was substantially lower than *amha* at all observed timepoints pre- and post-hatch (Fig 7B). This difference was still present after scaling read counts for differences in transcript length which is not accounted for by normalized read counts (Table S3). We found *amhy* expression trended towards higher expression at later developmental stages, consistent with a role in sex determination. However, this difference was not significant (anova p = 0.0769). We then hypothesized that male sex determination could be initiated by a higher overall dose of *amhy* when expressed simultaneously with *amha.* We compared *amha* and transcript length adjusted *amhy* normalized read counts at each stage and found no significant difference in total *amh* dosage between males and females at any timepoint (Table S3), suggesting dosage alone is not a mechanism for initiating male differentiation. Combined, our results indicate the unique regulatory elements that evolved for *amhy* do not increase early expression of *amhy*. Instead, they may alter expression level of *amhy* at other developmental stages and/or change spatial expression patterns, contributing to its new function in sex determination.

Sex differentiation genes are not differentially expressed between males and females early in development

Following sex determination, we expected to see divergence in the expression of overall male and female transcriptomes. However, principal component analysis of autosomal gene expression indicated that male and female larvae had similar expression profiles. Autosomal genes were clustered by developmental time rather than separating by sex at any stage of development (Fig 7A). Only sex chromosomes showed clear separation by both sex and developmental time (Fig S8), since the X chromosome is expressed two-fold higher in females,

relative to males, and the Y chromosome is only expressed in males. The overall lack of sex-specific expression on the autosomes suggests that many aspects of sex differentiation occur well after the earliest noted phenotypic difference between males and females: the proliferation of germ cells in the primordial gonad at 3 to 4 dah [81].

We examined whether any developmental stages had genes that were significantly differentially expressed between males and females. Many male and female differentiation genes are highly conserved across vertebrates [2] and should also be expressed during development of the threespine stickleback. For instance, we expected differential expression of key transcription factors canonically involved in differentiation, including the male biasing factors *dmrt1* and *sox9b* or the female biasing factors *foxl2a*, followed by divergence of downstream genes such as the aromatase enzyme *cyp19a1a* and the TGF-b hormones *amha* and *gsdf*. In total, we found 464 differentially expressed genes (DEGs) between males and females on the autosomes (File S1). Key regulators of differentiation should be differentially expressed throughout development and into adulthood in order to actively maintain gonadal fate [2]. However, 438 of the DEGs were only differentially expressed in a single stage (File S1), suggesting these genes do not play a substantial, ongoing role in sex differentiation. Additionally, while we expected to see an increase in the number DEGs over time due to activation of male and female specific gene networks, the number of DEGs was highest at stage 17 (152 DEGs), decreasing in later stages until a small increase from 4 dah (40 DEGs) to 8 dah (72 DEGs) (Fig S9). None of the canonical differentiation genes of interest were differentially expressed between males and females at any timepoint examined in this study (Fig 7). Male differentiation genes *dmrt1* and *amha* and female differentiation genes *foxl2* and *cyp19a1a* were differentially expressed in adult gonads of both wildtype and sex reversed fish, indicating their function in differentiation are conserved (Fig 2, Fig S4, Fig S7). Of the identified DEGs, only a small handful have known associations with gonadal function, development, or differentiation. Two genes associated with germ cell specification and maintenance [82], *ddx4* and *piwil1*,

325 showed female biased expression at 8 dah (Fig 2C). Interestingly, *amhrII,* which shows female
326 biased expression in embryonic mouse gonads [83], was also expressed more highly in females
327 at 8 dah. Although *cyp19a1a* was not differentially expressed, the steroidogenic enzyme
328 *hsd17b1*, which plays a role in estrogen activation [84], showed female biased expression at 8
329 dah. This gene acts as the SD gene in *Seriola* fishes [85] and is upregulated in ovaries of
330 Siberian sturgeon before the activation of *foxl2* or *cyp19a1a* [86]. A lack of differential
331 expression in many of these key genes indicates that gonad differentiation occurs after 8 dah.
332 We identified some other DEGs that have known reproductive functions in other
333 vertebrates but do not have clear connections to sex differentiation and are only differentially
334 expressed at a single timepoint. Gonadotropin-releasing hormone II receptor (LOC120811940)
335 has known roles in the stimulating steroidogenesis in both testes and ovaries across mammals
336 [87] and had male biased expression at stage 17 (logFC = 2.74, adjusted P = 1.4E-3). TGF-beta
337 3 hormone is expressed more highly in male mice during gonadogenesis [88], and a TGF-beta 3
338 proprotein like gene (LOC120807995) was expressed slightly higher in females at stage 17
339 (logFC = -0.63, adjusted P = 0.044). *Piwil2*, another germ cell associated gene [82], was
340 expressed higher in males at stage 20 (logFC = 1.72, adjusted P = 3.2E-3). *Cdc25b* is
341 expressed at low levels in mouse ovaries and testes [89] and was male biased at stage 23
342 (logFC = 0.52, adjusted P = 0.012). Separin/separase (*espl1*) has known roles in mitotic and
343 meiotic chromosome segregation [90] and was expressed at higher levels in 8 dah females
344 (logFC = -0.56, adjusted P = 1.2E-4). Additional work will be necessary to understand what
345 function, if any, these genes have in threespine stickleback gonad development.
346
347 **Discussion**
348 ***amhy* is the sex determination gene in threespine stickleback fish**
349 Our findings demonstrate that *amhy* is the SD gene in threespine stickleback, as it is
350 both necessary and sufficient for sex determination (Table 3). Independently derived *amhy*

351 genes have been functionally demonstrated to have a role in sex determination in three other
352 clades of teleost; however, threespine stickleback offers a novel perspective as their *amhy* is
353 more diverged, and genetic sex determination is more canalized in this species. Nile tilapia and
354 Japanese flounder have only one and nine SNPs, respectively, that differentiate their X- and Y-
355 linked copies of *amh* [15,16], and *amhy* in Patagonian pejerry shares 94% nucleotide identity
356 with its autosomal paralog [13]. In all three of these species, genetic sex determination can be
357 overridden to varying degrees by temperature [91–93]. In contrast, the threespine stickleback,
358 *amha* and *amhy* only share 78% nucleotide identity (Table 1). There is no evidence that
359 temperature can disrupt sex determination in threespine stickleback, and occurrences of sex
360 reversed or intersex stickleback in wild populations is rare [94,95]. This indicates that genetic
361 sex determination is highly canalized in threespine stickleback and less susceptible to
362 environmental signals that many other teleost species, making stickleback a robust model to
363 investigate how *amh* regulates gonadal development. Comparative studies across these taxa
364 will be invaluable for understanding how *amh* repeatedly evolves this novel function, and the
365 presence of an independently derived male associated *amh* duplication in the closely related
366 brook stickleback [22,40] makes the stickleback family an especially powerful tool for studying
367 the convergent evolution of *amh* as an SD gene.
368
369 **Potential mechanisms of sex determination in stickleback**
370 Germ cell density has been shown to affect sex determination in several teleost species,
371 with the male fate associated with lower germ cell count and the female fate with a higher count.
372 Common lab zebrafish strains are undifferentiated gonochorists, where all individuals begin
373 ovary development, but the gonad transitions early in males to a testis [96]. Complete ablation
374 of germ cells causes zebrafish to undergo male development [97], and a threshold of germ cells
375 at the time of gonadal differentiation is necessary to sustain ovary development [98]. *O. latipes*,
376 like sticklebacks, are differentiated gonochorists where either testis or ovary development

377 begins from a common undifferentiated primordium [99]. Ablation of germ cells in XX *O. latipes*
378 causes female-to-male sex reversal [100], and overproliferation of germ cells in XY fish causes
379 male-to-female sex reversal [101]. The association of germ cells with sex has also been
380 observed outside of teleosts in the red eared slider turtle (*Trachemys scripta elegans*) which has
381 temperature dependent sex determination. Embryos incubated at female promoting
382 temperatures have higher germ cell counts than those incubated at male promoting
383 temperatures, and depleting germ cells at intermediate temperatures biased the sex ratio
384 towards males [102]. This suggests the presence of a widely conserved, ancestral mechanism
385 in vertebrates by which germ cell density governs gonad differentiation. A new duplication of
386 *amh* could increase overall *amh* dosage, reducing germ cell proliferation to co-opt this
387 underlying mechanism and become a male determining gene.

388 Consistent with this mechanism, we found evidence that *amhy* is expressed in
389 threespine stickleback when germ cell proliferation diverges in males and females. While *amhy*
390 levels were low at all stages observed, *amhy* expression was highest in post hatching stages
391 where differences in germ cell proliferation between males and females are first observable in
392 the developing gonad [81]. We also found increased expression of germ cell specific genes (e.g.
393 *ddx4* and *piwil1*) in females at 8 dah, corroborating previous histological observations of
394 increased germ cell proliferation in female stickleback gonads beginning at 3 dah [81].
395 Overexpression of *amh* in mice [103] and chicken [104] causes reduced germ cell count and
396 gonad size. Studies misexpressing *amh* in telesots have primarily focused on sex determination;
397 however, gonadal hypertrophy observed in *amh* knockouts in other teleosts [32,34] alongside
398 gonadal hypotrophy with a lack of mature germ cells observed in some XX *Tg(amhy,EGFP)*
399 males in this study demonstrate the conserved function of *amh* suppressing germ cell
400 proliferation in stickleback and other teleosts.

401 Somatic cells may also be affected by *amhy* in other ways. In mice, low concentrations
402 of Amh promote proliferation and growth factor production in somatic cells, but increased

403 concentrations induce apoptosis [105]. Altering somatic cell proliferation could lead to
404 differences in the levels of hormones and growth factors that they produce, shaping gonadal
405 development. While Amh is not necessary for initial gonadal differentiation, it is important to
406 maintaining Sertoli cell fate in fetal mice [106]. Estrogen production in somatic cells also plays a
407 major role in sex differentiation and ovary development in teleosts (reviewed in [107,108]). In
408 tilapia, Amh signaling directly inhibits *cyp19a1a* production via Smad transcription factors [109].
409 While we did not detect a difference in *cyp19a1a* expression between males and females in
410 embryos or larvae, it was expressed more highly in adult ovaries than in testes, so *amhy* could
411 play a reinforcing role later in development to suppress estrogen synthesis in males. As we
412 were unable to isolate embryonic gonadal tissue for expression analysis, our results are
413 currently limited to characterizing total expression in the whole embryo. *Amh* can be expressed
414 in other developing tissues, such as the brain and heart [110,111]. If this is also the case in
415 threespine stickleback, this would obscure the true *amhy* to *amha* expression ratio in the gonad.
416 Further research characterizing the expression of *amha* and *amhy* in stickleback at spatial and
417 single cell levels will be essential for understanding how *amhy* functions in the developing
418 stickleback gonad.
419 The evolutionary changes that have given rise to novel function of *amhy* in stickleback
420 sex determination remain unclear. It is clear that substantial regulatory evolution has taken
421 place following the duplication of *amh* onto the Y chromosome; however, this regulatory
422 evolution has not led to earlier or higher expression of *amhy* relative to *amha* as we initially
423 predicted. While we suspect a more detailed study of *amha* and *amhy* expression at tissue and
424 cell specific levels will lend insight into the role of this regulatory evolution, we also should not
425 rule out the significance of coding sequence evolution for *amhy*. In Nile tilapia, *amhy* expression
426 is lower than the X-linked *amh* throughout development, and misexpression of *amhy* but not
427 *amh* induces male sex determination [16]. This implies that the single missense SNP between
428 *amh* and *amhy* in tilapia is important to the function of *amhy* in sex determination. In Spotted

429 knifejaw (*Oplegnathus punctatus*), a Y linked copy of *amhrII* shows higher affinity for binding
430 *amh* than its X linked paralog [23]. In zebrafish which lack *amhrII*, *amh* may instead use the type
431 II TGF-β receptor *bmpr2a* [112,113]. Mutations that increase the stability of Amhy, increase its
432 affinity for the receptor, AmhrII, or promote interaction with a non-canonical receptor could also
433 affect gonadal development.
434
435 **Sex differentiation occurs later than anticipated**
436 We observed no differential expression in canonical vertebrate sex differentiation genes,
437 including *dmrt1, sox9b, foxl2a,* and *cyp19a1a.* While the order and timing of expression varies
438 across taxa, these core genes are reliably differentially expressed between males and females
439 before the onset of morphological gonadal differentiation [114–116]. This indicates that there is
440 some delay between the initial establishment of germ cell differences between males and
441 females and the later differentiation of the primordial gonad into either a testis or ovary.
442 Expression analysis of whole embryos and larvae could obscure gonad specific changes in
443 gene expression as previously discussed. However, we did identify differential expression of
444 *ddx4* and *piwi1l* which are highly germ cell specific [82] as well as *hsd17b1* and *amhrII* which
445 are not gonad specific [84,111] but show early female biased gonadal expression in other
446 species [83,86]. This demonstrates some ability to detect sex differences in expression for
447 significant genes. We propose that sex determination in threespine stickleback occurs in two
448 phases. In the early critical period of sex determination, germ cell proliferation in the
449 undifferentiated gonad diverges between males and females due to the presence of *amhy* in
450 males. Then, during the sensitive period of gonadal differentiation, the difference in germ cell
451 count between males and females dictates gonadal fate, marking the end of the sex
452 determination and the beginning of differentiation. Unlike *Sry* in mammals which is expressed in
453 a brief window and directly initiates gonadal differentiation [117], *amhy* in stickleback appears to
454 be expressed throughout this early period of germ cell proliferation. These two phases of germ

455 cell proliferation followed by gonad differentiation are also present in other species with SD
456 genes including Nile tilapia (reviewed in [118]), and medaka (reviewed in [99]) as well as
457 species without SD genes such as red eared slider [102] where germ cell proliferation is
458 affected by temperature. This suggests that this two-phase system of differential germ cell
459 proliferation followed by gonadal differentiation is broadly conserved across vertebrates, but
460 what combination of environmental and/or genetic factors influences germ cell proliferation has
461 changed between taxa. The ability of *amh* to immediately integrate with this preexisting sex
462 determination network through its existing function in regulating germ cell proliferation along
463 with possible reinforcing roles in regulating somatic cell identity and estrogen synthesis would
464 explain the prevalence of *amh* as an SD gene.
465
466 **Fertility of sex reversed threespine stickleback**
467 Both XY *amhy*-KO females and XX *Tg(amhy,EGFP)* male sex reversed fish were fertile
468 in our study. Fertility of sex reversed mutants is not uncommon in other teleost species;
469 however, it is often observed in species with younger or less diverged sex chromosomes. In
470 these instances, the X and Y chromosomes contain a similar complement of genes. In medaka,
471 the Y specific region is 280 kb and the only functional gene it contains is the sex determining
472 *dmrt1by* [12]. In Nile Tilapia, the sex determining region on linkage group 23 is 1.5 Mb and
473 contains 51 annotated genes, including the sex determining *amhy* [119]. In both species, sex
474 reversed fish are fertile and YY offspring are viable [11,120]. In contrast, the threespine
475 stickleback Y chromosome has a ~15 Mb non-recombining region [20]. Within this region, the Y
476 chromosome has lost half of the almost 1200 ancestral gametologs, causing inviability of YY
477 embryos, and has accumulated many Y-specific genes not present on the X chromosome [20].
478 Sex chromosome-specific gene content evolution could lead to improper expression in the
479 opposite sex, affecting gametogenesis. Given this divergence, the ability of both XY *amhy*-KO
480 females and XX *Tg(amhy,EGFP)* males to reproduce is surprising. In mouse, reduced fertility of

481 XY females is a result of meiotic errors between the X and Y chromosomes as well as the effect
482 of aberrant Y-chromosome genes in the ooplasm on early development (Reviewed in [121]). As
483 clutch size in XY females did not differ from XX siblings and some crosses from XY females
484 have normal viability, it seems unlikely that widespread meiotic failure occurs in XY female
485 stickleback. Furthermore, it is clear that Y chromosome transcripts or dosage differences from X
486 chromosome genes do not prevent embryo development. Threespine stickleback are batch
487 spawners that produce multiple clutches of eggs over a single breeding season [77]. If ovulated
488 eggs are not passed, they can become overripe and inviable [122,123]. Overripe eggs can also
489 harden and obstruct the fish, causing them to become eggbound. Many of the clutches from XY
490 *amhy*-KO females had this hardened, overripe appearance that is uncommon in our lab-reared,
491 wildtype fish. In addition, some XY females we attempted to cross had no cloaca dilation and
492 were eggbound. We suspect that subfertility of XY females is not due to an inability to produce
493 viable eggs, but due to an inability to pass these eggs once mature. Whereas wildtype fish can
494 pass eggs on their own and begin another cycle of ovulation, XY females retain these eggs until
495 they are manually removed. Repeated and frequent crossing would prevent overripe eggs from
496 building up and allow the harvest of freshly ovulated, viable eggs. Hormones produced by the
497 gonad and pituitary gland appears to play a role in egg maturation and overripening for
498 stickleback [123,124], so while XY females are histologically similar to XX females, variation in
499 hormone production could inhibit proper production and release of eggs.

500 The mammalian Y chromosome has several genes essential for spermatogenesis and
501 sperm development [125–129]. Single cell sequencing has shown that many Y-specific genes
502 are expressed throughout spermatogenesis in stickleback [130], but these genes are apparently
503 not essential for this process. Several XX *Tg(amhy,EGFP)* males from this study had testes with
504 many fully mature spermatozoa that were able to fertilize eggs and generate viable progeny at
505 similar rates to wildtype sperm. This raises a question of the importance of the Y chromosome
506 to fitness and reproduction. Testes from fertile XX males did not show an obvious reduction in

sperm number indicating that widespread meiotic arrest does not occur in XX males. Stickleback are external fertilizers in which sperm competition frequently occurs [131]. Variation in sperm morphology [132] and motility [133] can contribute to reproductive success, so there may be differences in sperm function that our *ex vivo* fertilization assays do not capture. Some XX *Tg(amhy,EGFP)* males did have hypotrophic testes with a reduction in identifiable germ cells, but since this phenotype was not universal, we suspect that variation in transgene copy number and insertion location led to overexpression of *amhy* in these fish. The germline *Tg(amhy,EGFP)* offspring we produced will allow us to determine if this phenotypic variation exists in a consistent genetic background.

A four core genotypes stickleback model

Sex chromosomes impact a wide range of traits outside of fertility that are still critical to fitness. By comparing XY males and XX females to sex reversed XY females and XX males, the four core genotypes mouse model has allowed researchers to dissect the role of genotypic and gonadal sex to a number of behavioral and physiological sex differences in mammals (reviewed in [134,135]) including mating behavior [136] and parental care [137]. The creation of reproductively mature XX males and XY females in this study offers a new vertebrate model to study the separate contributions of gonadal sex and sex chromosomes to sexual dimorphism.

Many traits are sexually dimorphic in the threespine stickleback, including shape and size of the head and body [43–46], bony armor features [43,44], and brain size [47,48] as well as feeding behaviors [49,50] and boldness [51]. Male stickleback also show complex courtship and mating behavior [52,53] and male-only paternal care [54], and females show a variety of mate choice preferences [55–60]. Male nuptial coloration is a particularly interesting trait, as strong coloration is beneficial for courtship [60,61], but has a cost of increased risk of predation [62,63]. Therefore, sexually antagonistic selection would select for stronger, more conspicuous coloration in males and inconspicuous coloration in females. Androgens, secreted from the

533 gonads, are shown influence nuptial coloration in stickleback [64]. These observations are
534 supported by the presence of nuptial coloration in XX males in our study, which lack all Y-linked
535 genes, but have functioning testes. In contrast, male nuptial coloration in XY females that lack
536 testes shows that there are also Y-linked factors that contribute to nuptial coloration independent
537 of gonadal sex. Future research with the four core genotypes stickleback will provide many
538 insights into the genetic basis of sexual dimorphism and how sexually antagonistic selection
539 shapes the evolution of sex chromosomes.
540

541 **Methods**

542 All experiments used lab-derived progeny from wild-caught threespine stickleback fish
543 from Port Gardner Bay (Washington, USA) and Japan Pacific Ocean (Akkeshi, Japan). All
544 procedures were approved by the University of Georgia Animal Care and Use Committee
545 (protocols A2021 07-031-Y3 and A2024 08-009-Y1). We collected fish from Washington State
546 over multiple years using Scientific Collection Permit numbers 21-122, 22-150, 23-147, and 24-
547 143.
548

549 **CRISPR/Cas9 knockout of *amhy***

550 We microinjected stickleback embryos following standard procedures [41], with the
551 addition of KCl to the injection mix at a final concentration of 0.2 M [138]. Cas9 protein was
552 purchased from QB3 MacroLab (University of California, Berkeley). Synthetic sgRNAs were
553 designed using CHOPCHOP [139–141] and purchased from Synthego: amhy_sgRNA_77r (5'-
554 GATCAGCTGCTGTCCATGCA-3') and amhy_sgRNA_600r (5'- GGTCCTCTCTCGTCTTCGTT -
555 3'). We combined Cas9 protein and sgRNA at a final concentration of 10 μM each and
556 incubated for at least ten minutes at room temperature to allow the ribonucleoprotein (RNP) to
557 form. The injection mix was made to a final concentration of 4 μM RNP.
558

559 **Synthesis of constructs and transgenesis**

560 Plasmids pBT2 [142], pUbi:Switch [75], and pCS-zT2TP [8] were kindly shared by Mary
561 Goll. Plasmid pT2AL200R150G [71] (referred to as pT2Xla.Ef1a:EFGP) was kindly shared by
562 Tyler Square and Craig Miller. We purchased a synthetic amhy,EGFP construct from TWIST
563 Bioscience (San Francisco, CA, USA). This construct consisted of a Kozak consensus
564 sequence (5'-GCCGCCACCATGG-3'), N-terminus flag tag, the threespine stickleback *amhy*
565 coding sequence, a P2A self cleaving peptide [73,74], EGFP, and an SV40 poly(A) sequence,
566 all flanked by 5' BamHI and 3' NotI restriction sites to facilitate cloning. We performed all
567 restriction digests were following the manufacturer's guidelines (New England Biolabs). We
568 isolated all of the plasmids using a Monarch Plasmid Miniprep Kit (NEB #T1010) and gel
569 purified all DNA fragments using the Monarch Gel Extraction kit (NEB #T1020). DNA fragments
570 were ligated using T4 DNA Ligase following manufacturer recommended protcols (NEB
571 #M0202). We transformed all plasmids into DH10B competent cells (Thermo Scientific EC0113).
572 All plasmids were sequenced by Azenta Life Sciences (South Plainfield, NJ, USA) (File S2).

573 We assembled each construct as follows:

574 1. pT2Dre.Ubi:amhy,EGFP: The *D. rerio* ubiquitin promoter was excised from
575 pUbi:Switch and cloned into pBT2 using XhoI and BamHI. The synthetic amhy,EGFP
576 construct was excised from pTwist_amhy-P2A-EGFP and cloned into the
577 intermediate pT2Dre.Ubi backbone using BamHI and NotI.
578 2. pT2Dre.Ubi:EGFP: the *D. rerio* ubiquitin promoter was excised from pUbi:Switch and
579 cloned into pT2Xla.Ef1a:EGFP using XhoI and BamHI.
580 3. pT2Xla.Ef1a:amhy,EGFP: the synthetic amhy,EGFP construct was excised from
581 pT2Dre.Ubi:amhy,EGFP and cloned into pT2Xla.Ef1a:EGFP using BamHI and BglII.
582 4. pT2-5amhy2.5,Xla.Ef1a:EGFP: an 11.5 kb region of the Y chromosome containing
583 *amhy* along with 5 kb of upstream and 2.5 kb downstream DNA was excised from
584 bacterial artificial chromosome STB26-N21 from the CHORI-215 library [143] and

585 cloned into pBT2 using BamHI and XhoI. The Xla.Ef1a:EGFP cassette was excised
586 from pT2Xla.Ef1a:EGFP by digestion with XhoI and HpaI and ligated into the
587 intermediate pT2-5amhy2.5 plasmid following digestion with XhoI and SwaI.
588 We synthesized Tol2 mRNA using the mMessage mMachine SP6 Transcription kit
589 (Invitrogen AM1340) and purified the product with the MEGAclear Transcription Clean-Up Kit
590 (Invitrogen AM1908). We injected stickleback embryos were as in [41] with the addition of KCl to
591 a final concentration of 0.2 M [138]. All embryos were screened for EGFP expression five to
592 seven days after injections before hatching had occurred. We removed all embryos without
593 discernable somatic EGFP fluorescence.
594
595 **Genotyping and sanger sequencing**
596 We extracted DNA from fin clips or whole embryos using a HotSHOT isolation protocol
597 [144]. We performed all PCR reactions on an Analytik Jena Biometra Tone in a total volume of
598 20 µl using 0.8 µL of genomic DNA, 0.2 µM each primer, 0.2 mM each dNTPs, 0.5 units
599 DreamTaq DNA polymerase (Thermo Scientific EP), and 2 µl 10x DreamTaq Green Buffer with
600 20 mM $MgCl_2$. We genotyped fish for sex using the sex-linked marker *idh* [39] with the following
601 cycling conditions: 1 cycle of 95°C for 2 min; 30 cycles of 95°C for 30 s, 57.3°C for 30 s, and
602 72°C for 30 s; 1 cycle of 72°C for 5 minutes. All other reactions used: 1 cycle of 95°C for 2 min;
603 35 cycles of 95°C for 30 s, 60°C for 30 s, and 72°C for 30 s; 1 cycle of 72°C for 5 minutes.
604 Primer sequences for all reactions are listed in Table S4. We purified the PCR product using a
605 Monarch PCR & DNA cleanup kit (NEB #T1030). All samples were Sanger sequenced through
606 Azenta Life Sciences (South Plainfield, NJ, USA).
607
608 **Phenotyping and crossing**
609 To phenotype gonads, we euthanized adult stickleback fish in 0.05% MS-222 buffered to
610 neutral. We dissected out the gonads and fixed one or both gonads for 24 to 48 hours in 10%

611 neutral buffered formalin. The remainder of the fish was preserved in 75% ethanol. The gonads
612 were processed, embedded in paraffin, sectioned at 5 µm, and stained with hematoxylin and
613 eosin by the University of Georgia College of Veterinary Medicine Histology Lab. We used a
614 Zeiss Axio Scope A1 microscope and Zeiss Axiocam 305 Color camera to capture all images at
615 the University of Georgia Biomedical Microscopy Core.
616 To make crosses, we euthanized mutant or wildtype male stickleback and gently
617 macerated testes in 500 µl of Hanks' Balanced Salt Solution. We stripped eggs from gravid
618 females and applied approximately 50 µl of sperm solution with a disposable transfer pipette.
619 We photographed adult stickleback with a Samsung Galaxy S22 under standardized lighting.
620
621 **Riboprobe synthesis**
622 We generated riboprobe templates for *gsdf, dmrt1, foxl2,* and *cyp10a1a* from cDNA from
623 adult gonads. We extracted total RNA from mature testis and ovary tissue using TRIzol Reagent
624 (Invitrogen 15596026) according to manufacturer's instructions. We synthesized cDNA using the
625 iScript cDNA Synthesis Kit (Bio-Rad 1708891) and amplified the targeted region for each gene
626 through PCR as described above (Table S4). We cloned the PCR product into plasmid pJC53.2
627 (kindly shared by Kendall Clay and Rachel Roberts-Galbraith) after digestion with Eam1105I
628 (Thermo Scientific FD0244) as in Collins *et al*. 2010 [145]. We verified each riboprobe template
629 after cloning with sanger sequencing by Azenta Life Sciences (South Plainfield, NJ, USA). For
630 *amha*, we ordered a synthetic gene fragment from TWIST Bioscience (San Francisco, CA, USA)
631 containing a 307 bp region of the *amha* cds flanked by a 5' T3 promoter and 3' T7 promoter to
632 facilitate riboprobe synthesis (File S2).
633 To synthesize riboprobes, we PCR amplified linear template from the appropriate
634 plasmid or used the synthetic gene fragment directly. We performed *in vitro* transcription from
635 these templates using T7 (New England Biolabs M0251S), T3 (New England Biolabs M0378S),
636 or SP6 (New England Biolabs M0207S) RNA polymerase according to manufacturer's

637 instructions, substituting 0.2 mM of UTP for DIG-labeled UTP (Roche 11209256910). We
638 purified riboprobes with a DNase treatment (New England Biolabs M0303S) and an ammonium
639 acetate precipitation.
640
641 ***In situ* hybridization**
642 We adapted a colorimetric *in situ* hybridization (ISH) protocol from Square, *et al.* 2021
643 [146]. We fixed the dissected gonads for 24-48 hours in 10% neutral buffered formalin. The
644 gonads were processed, embedded in paraffin, and sectioned at 5 µm by the University of
645 Georgia College of Veterinary Medicine Histology Lab. Unless otherwise stated, we performed
646 all steps in Lock-Mailer microscope slide jars in a volume of 9-11mL and at room temperature.
647 To deparaffinize, we warmed the slides in a 65°C incubator for five minutes, allowed them to
648 cool to room temperature, then washed the slides in Hemo-De once for 5 minutes then again for
649 10 minutes. We performed prehybridization washes indicated with an asterisk in a Tissue-Tek II
650 Slide Staining Station rather than Lock-Mailer jars: 100% EtOH for 5 minutes*, 80% EtOH for 10
651 minutes*, Milli-Q water for 10 minutes*, PBST for 5 minutes*, 15 ug/mL proteinase K in PBST
652 for 5 minutes, PBST rinse*, 4% PFA for 20 minutes, PBST twice for 10 minutes each*, 67°C pre-
653 heated hybridization buffer (50% formamide, 5X SSC, 0.1% Tween, 5mg/mL CHAPS, 0.1
654 mg/mL yeast RNA, 0.1mg/mL heparin, pH 6.0 with citric acid) twice for 5 minutes each, and pre-
655 heated hybridization buffer for 1 to 4 hours on a rotator at 67°C. We performed hybridization
656 with 100-500 ng/mL of riboprobe in hybridization buffer incubated overnight rotating at 67°C. We
657 stored hybridization solution at 20°C and reused up to 3 times.
658 Post-hybridization, we washed the slides 6 times with hybridization wash (50%
659 formamide, 5X SSC, 0.1% Tween) rotating at 67°C for 20-90 minutes each, totaling 5 to 6
660 hours. We rinsed the slides in MABT (maleic acid buffer with Tween) and washed them in MABT
661 for twice for 20 minutes each, first at 67°C, then at room temperature. We added blocking
662 solution (2% Blocking Reagent (Roche 11096176001) in MAB) to each slide, covered the slides

663 with parafilm, and incubated for 1 to 3 hours in a humidor. We poured off the blocking solution
664 and added 1:2000 anti-digoxigenin alkaline phosphate antibody (Roche 11093274910) in
665 blocking solution, covered the slides with parafilm, and left them in a humidor overnight at 4°C.
666 We performed five 20-50 minute post-antibody washes hybridization wash solution (50%
667 formamide, 5X SSC, 0.1% Tween, citric acid to pH 6.0) on a rotator for a total of three to four
668 hours, followed by an overnight MABT wash at 4°C.
669 Prior to coloration, we performed three 5-to-10-minute washes in NTMT (0.1 M NaCl, 0.1
670 M Tris pH 9.5, 0.05 M MgCl2, 0.1% Tween). We moved the slides into coloration solution
671 (blocking solution plus 25 ug/mL NBT and 175 ug/mL BCIP) and incubated 2 to 30 hours
672 covered to block light. We removed the slides from coloration solution once the color was stable
673 in the positive control (*gsdf*), but before any background color was seen in the negative control
674 (sense *gsdf*). Once coloration was complete, we rinsed the slides with PBST and washed for 10
675 minutes in PBST. We fixed the slides in 4% PFA in PBS at 4°C for one to five days.
676 To prepare slides for mounting, we performed three 5-minute washes in PBST and three
677 5-minute washes in deionized water. We mounted and coverslipped the slides using Vectashield
678 antifade mounting medium with DAPI. We used a Zeiss Axio Scope A1 microscope and Zeiss
679 Axiocam 305 Color camera to capture all images at the University of Georgia Biomedical
680 Microscopy Core.
681
682 **Sequence Alignments**
683 We retrieved sequences for *amha* (Gene ID: 120823390) and *amhy* (Gene ID:
684 120812167) from threespine assembly GAculeatus_UGA_version5 (GCF_016920845.1) and
685 *amh* (Gene ID: 119216504) from ninespine assembly fPunPun2.1 (GCF_949316345.1). We
686 performed all alignments and calculated sequence identity between *amh* homologues with
687 Muscle 5.1 [147] within Geneious Prime (v2024.0.5) using default parameters. We defined
688 intron and exon positions based upon the threespine *amha* sequence in each alignment. We

689 calculated dN/dS with the R package ape v5.8-1 [148] using the translation aligned coding
690 sequences of *amha* (XM_040183306.1)*, amhy* (XM_040167960.1), and ninespine *amh*
691 (XM_037469420.2). One additional base was included at the 5' end of exon 7 of the ninespine
692 *amh* cds in order to correct the predicted annotation which contains multiple premature stop
693 codons in this final exon. Alignment files are presented in File S2. We generated Vistaplots
694 [149,150] using LAGAN [151] alignments and a 100 bp window size with a 70% sequence
695 identity threshold.
696
697 **RNAseq**
698 We staged embryos according to established stickleback developmental stages [80] and
699 preserved the whole embryos in RNAlater Stabilization Solution (Invitrogen AM7021) following
700 manufacturer guidelines and stored at -80 °C until analysis. We extracted RNA using TRIzol
701 Reagent (Invitrogen 15596026) and the Direct-zol RNA Microprep Kit (Zymo R2062). We
702 created sequencing libraries using the Illumina TruSeq Stranded mRNA Library Prep kit
703 (20020594). We pooled the libraries from all samples and 150 bp paired end reads were
704 sequenced on two lanes using a NovaSeq X Plus by Azenta Life Sciences (South Plainfield, NJ,
705 USA). All of the samples were sequenced to an average of 34.7 M read depth (min 11.6 M, max
706 71.3 M, SD = 10.4 M) (File S1). We trimmed raw reads for quality and sequencing adapters with
707 Trimmomatic (v. 0.39) [152] using leading and trailing quality threshold of 3, a sliding window of
708 4 with quality threshold of 15, and minimum length cutoff of 36. We aligned paired and orphan
709 reads to the threespine stickleback reference genome (GAculeatus_UGA_version5, NCBI
710 RefSeq assembly GCF_016920845.1) using HISAT-3N [153] with default parameters. All
711 samples had an alignment rate between 73% and 92% (File S1). We generated Indexed BAM
712 files of the alignments with Samtools (v. 1.17). We generated transcript counts against the NCBI
713 annotation GTF file (release 100) for GCF_016920845.1 with HTseq (v. 2.0.2) [154] using
714 HTSeq-count with default parameters except --stranded=no. We performed all remaining

715 analyses in R (v. 4.4.1) and RStudio (v. 2024.04.2+764). We combined the counts from paired
716 and orphaned reads for each sample and used DESeq2 (v. 1.44.0) [155] to generate normalized
717 read counts and perform differential expression analysis. We identified DEGs using the standard
718 workflow with stage and sex combined as a single factor. We used the contrast function to
719 calculate log2 fold changes (logFC) and adjusted p values for differential expression between
720 males and females at each timepoint. We identified DEGs of interest using GO terms from the
721 NIH gene2go database (https://ftp.ncbi.nlm.nih.gov/gene/DATA/).
722

723 **Material Availability**

724 RNAseq data is available in the NCBI SRA under BioProject PRJNA1248589. Raw and
725 normalized read counts are available in the NCBI GEO under accession GSE296766. All scripts
726 are available at https://github.com/MTreasterUGA/Amhy-sex-determination. All plasmids are
727 available upon request.
728

729 **Acknowledgements**

730 This work was funded by the National Science Foundation MCB 1943283 (M.A.W), the National
731 Institutes of Health 1T32GM142623 (M.J.T.), The University of Georgia Research Foundation
732 (M.J.T.), the Society for the Study of Evolution R.C. Lewontin Early Award (M.J.T.), and ARCS
733 Foundation (M.J.T.).
734 Research reported in this publication was supported by the National Institute of General Medical
735 Sciences of the National Institutes of Health under Award Number R01GM147312 (M.A.W). The
736 content is solely the responsibility of the authors and does not necessarily represent the official
737 views of the National Institutes of Health.
738 This study was supported in part by resources and technical expertise from the Georgia
739 Advanced Computing Resource Center, a partnership between the University of Georgia's

Office of the Vice President for Research and Office of the Vice President for Information Technology.

The imaging data used in this publication was produced in collaboration with the Biomedical Microscopy Core at the University of Georgia.

We thank Koichi Kawakami (National Institute of Genetics, Japan) for use of the Tol2 elements in this study.

Declaration of Interests

The authors declare no conflicts of interests

750 **Figures**

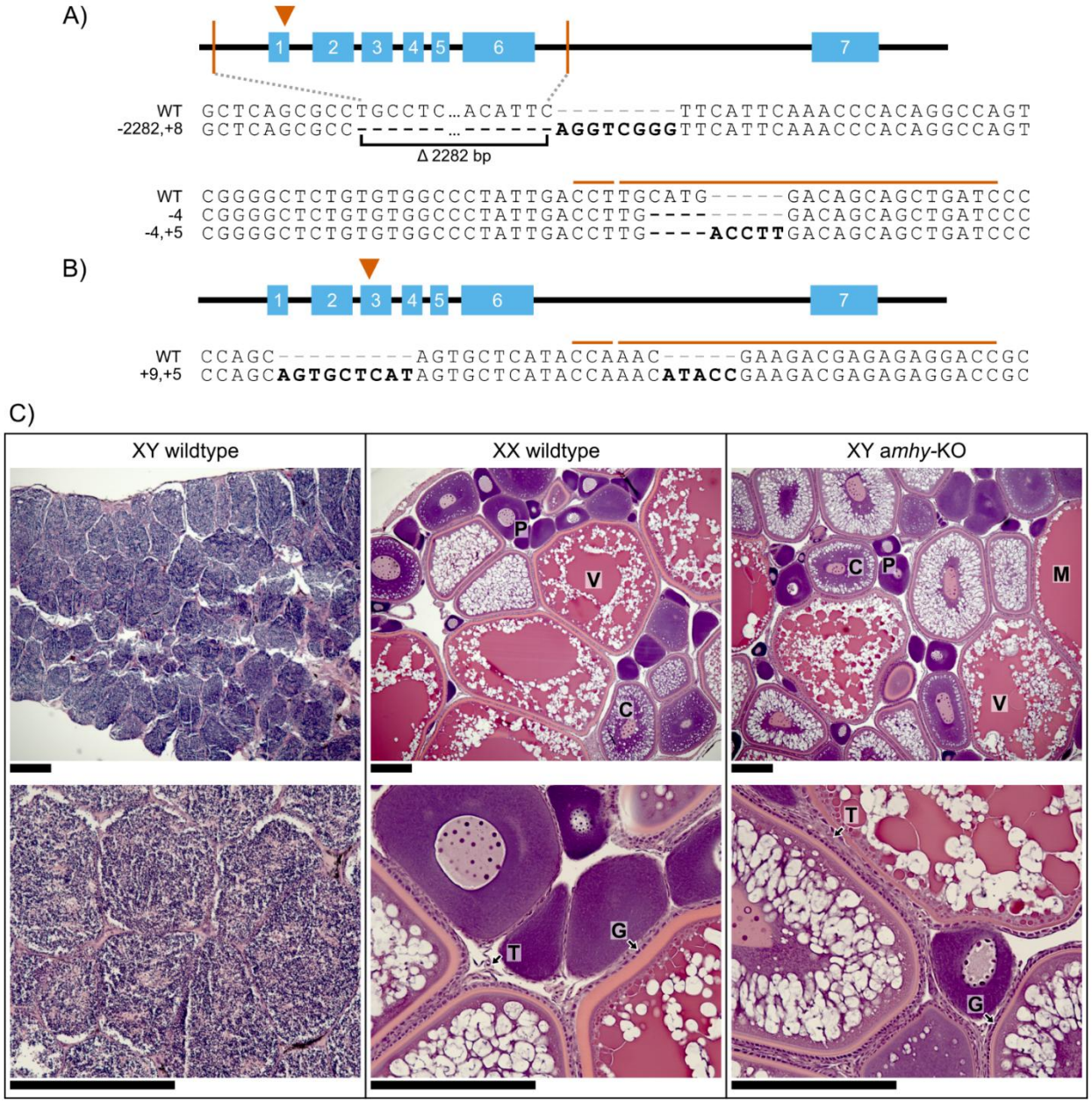

751

752 Fig 1. CRISPR/Cas9 knockout of *amhy* caused male to female sex reversal in F1 XY fish.

753 We used CRISPR/Cas9 to target exon 1 (A) or exon 2 (B) of *amhy*. CRISPR target site and

754 PAM sequence are indicated by orange lines above wildtype reference sequence. Mutations

755 relative to wildtype are bolded. We identified four loss of function *amhy* alleles in F1 progeny.

756 One allele (-2282,+8) deleted the first six exons of *amhy*. Other alleles featured small frameshift

757 indels. C) We identified male to female sex reversal using gonad morphology and histology.
758 Ovaries in XX wildtype and XY *amhy*-KO fish feature oocytes throughout multiple stages of
759 development. P – primary oocyte, C – cortical alveolus stage V – vitellogenic stage, M – Mature
760 oocyte, G – Granulosa cells, T – Theca cells. Scale bars = 200 µm.
761

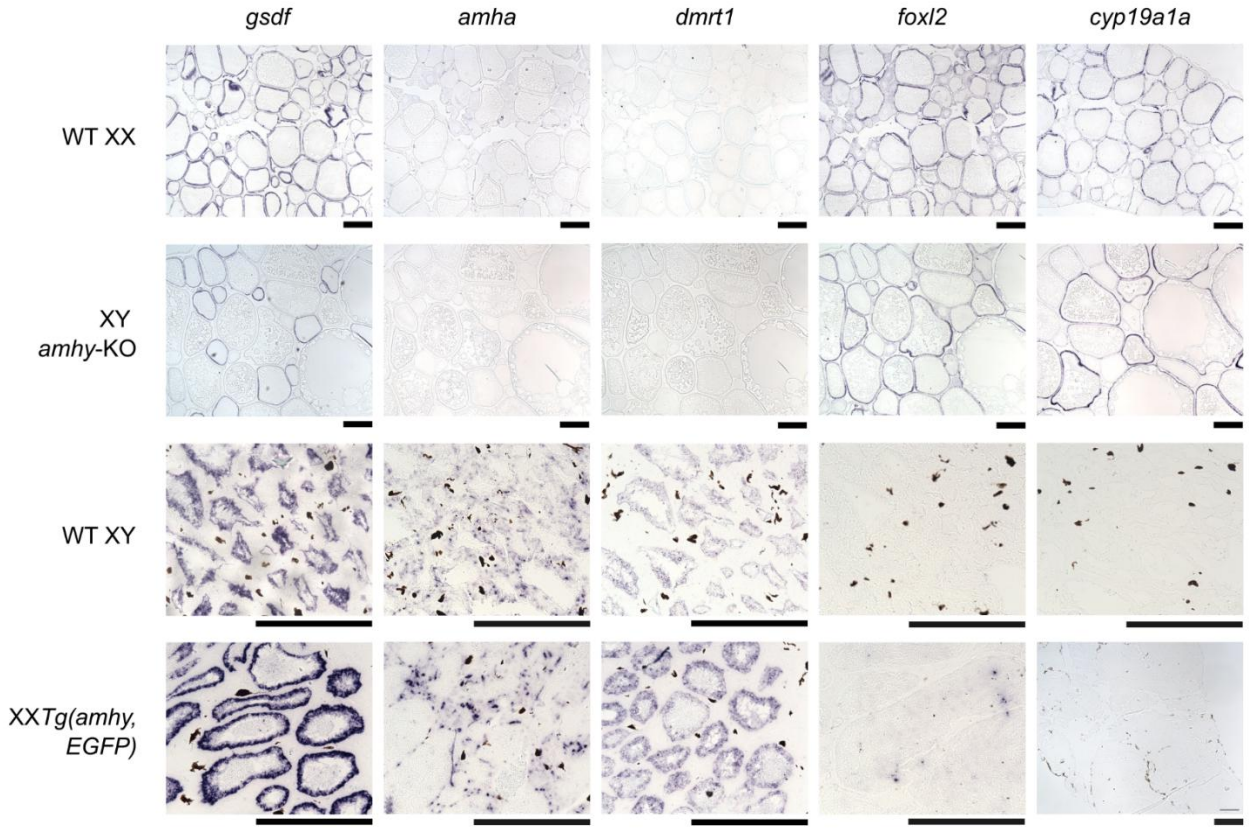

762
763 Fig 2. Gene expression in sex reversed gonads resembles expression in wild type gonads.
764 *In situ* hybridization of gonadal genes in wildtype and sex reversed stickleback gonads. A
765 positive control gene *gsdf* was expressed in somatic cells of both testes and ovaries. Wildtype
766 XY and sex reversed XX testes show strong expression of male differentiation genes *amha* and
767 *dmrt1* but not female differentiaiton genes *foxl2* and *cyp19a1a*. Wildtype XX and sex reversed
768 XY ovaries strongly express female differentiation genes but not male differentiation genes.
769 Scale bars = 200 µm.
770

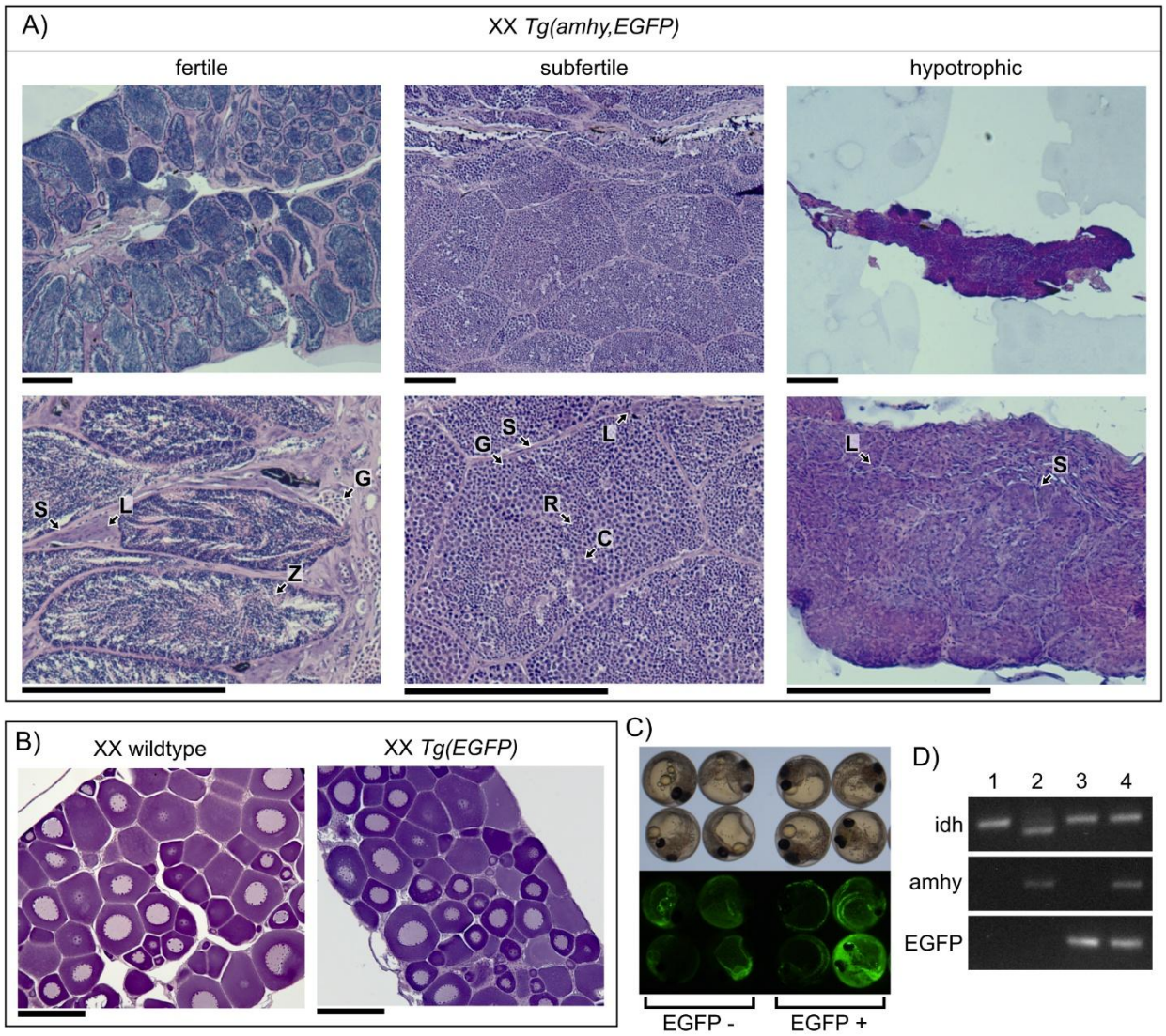

Fig 3. XX fish with an *amhy* transgene exhibit female to male sex reversal.

A) XX *Tg(-5amhy3.5,Xla.Ef1a:EGFP)* fish developed testes with varying cell composition. Fertile and subfertile fish had testes with clearly defined cysts of synchronously developing sperm. Hypotrophic testes did not have discernable germ cells. G – spermatogonia, C – spermatocyte, R – round spermatid, Z – Spermatozoa, L – Leydig cells, S – Sertoli cells Scale bars = 200 μm. B) Control XX *Tg(Xla.Ef1a:EGFP)* fish developed ovaries identical to wildtype XX counterparts. Scale bars = 200 μm. C) Embryos injected with pT2-5amhy3.5,Xla.Ef1a:EGFP seven days after fertilization under bright field (top) and EGFP excitation (bottom). Embryos positive for transgene integration show somatic EGFP expression. We removed embryos with no EGFP

expression or EGFP expression only in the yolk, which indicates the yolk was injected rather than the blastomere [41]. D) We used PCR of the sex-linked marker *idh* to genotype XX and XY fish. PCR of EGFP and *amhy* show the presence of the associated transgene. 1 – wildtype XX, 2 – wildtype XY, 3 – XX *Tg(EGFP)*, 4 – XX *Tg(amhy,EGFP)*.

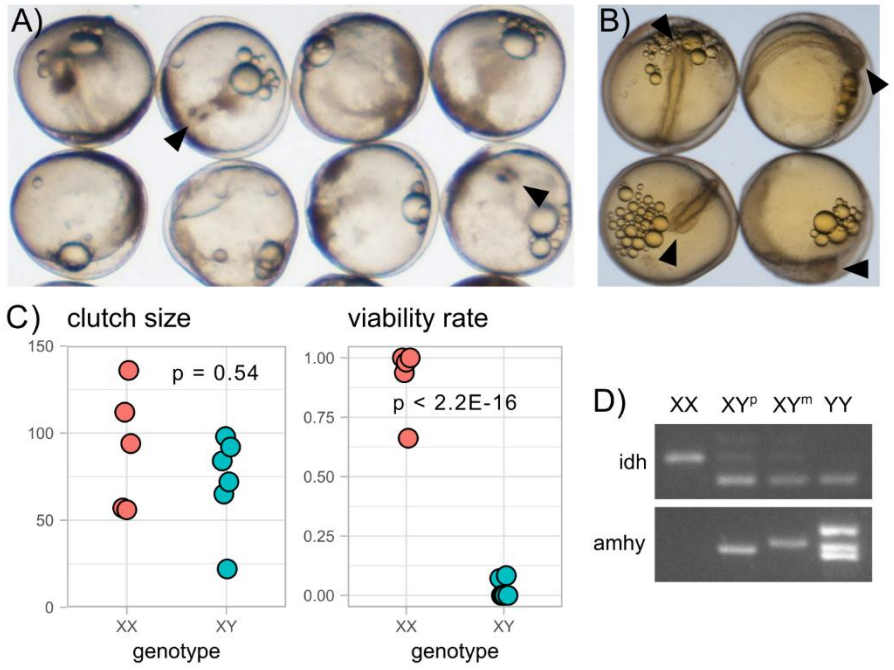

Fig 4. XY *amhy*-KO females can reproduce and transmit an X or Y chromosome. YY embryos (A) at 48 hours post fertilization show arrested development compared to wildtype embryos (B). Arrowheads denote anterior end of body axis. C) F2 XX and XY *amhy*-KO female siblings do not show a significant difference in clutch size (wilcoxon test, $p < 0.05$). Clutches from XY *amhy*-KO females have a significantly lower viability rate than those from XX female siblings (z test, $p < 0.05$). D) PCR of the sex linked marker IDH shows the absence of the X chromosome in YY embryos. Both the paternal (wildtype) and maternal (+9,+5) loss of function alleles can be detected in XY offspring. YY embryos show the presence of both amhy alleles as well as a third band, likely a heterodimer of the maternal and paternal amplicons.

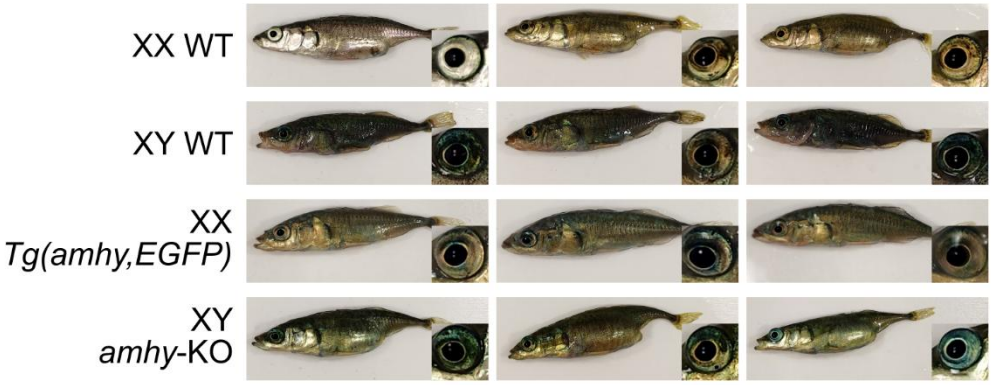

Fig 5. Both male and female sex reversed stickleback show partial male nuptial coloration. Wildtype XX females are silver and may darken slightly when gravid. Wildtype XY males have dark blue eyes and bodies and red throats. Sex reversed XX *Tg(amhy,EGFP)* males are less dark than wildtype males but show blue coloration on the body and eyes. Sex reversed XY *amhy*-KO females show slight or moderate darkening of the body with distinct blue eyes not typical of wildtype XX females.

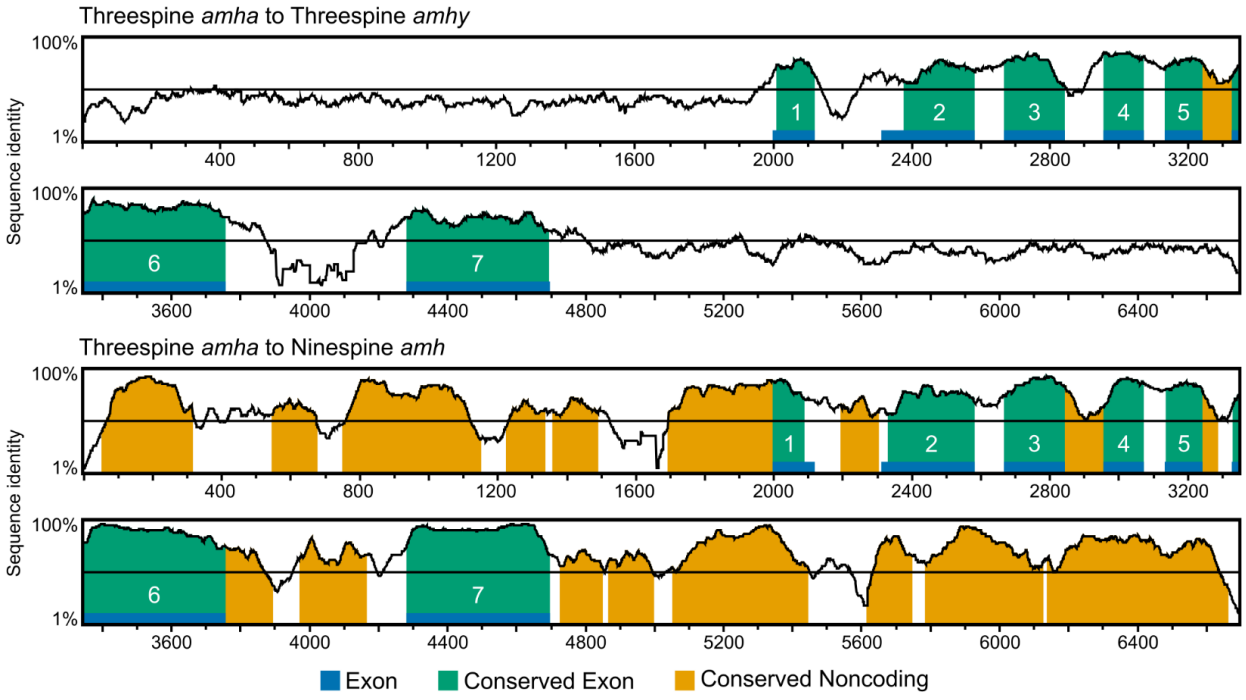

Fig 6. *amha* and *amhy* show no sequence conservation outside of the coding sequence.

807 Vistaplots showing conserved sequence identity of threespine *amha* to threespine *amhy* (top)
808 and to ninespine *amh* (bottom) with sequence identity on the y axis and nucleotide position of
809 threespine *amha* on the x axis. Exon positions are indicated along the x axis in blue. Conserved
810 exon and noncoding sequences share 70% sequence identity in a 100 bp window.
811

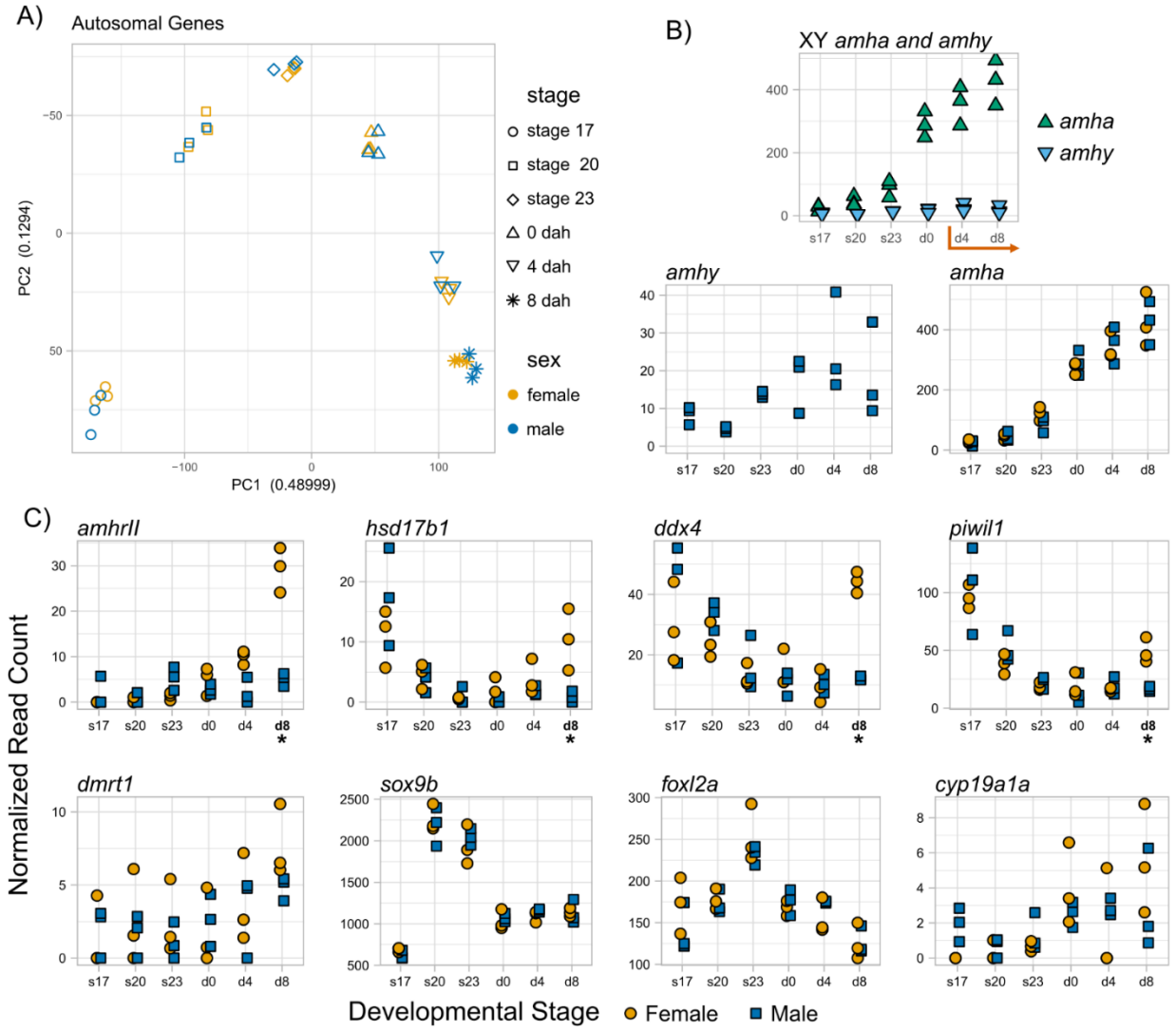

812
813 Fig 7. Expression of gonadal growth and differentiation genes in embryonic and larval
814 stickleback.
815 (A) PCA plots of normalized read counts for all genes cluster by stage rather than sex. (B) and
816 (C) Normalized read counts of genes in embryonic stages 17, 20, 23, and larvae 0, 4, and 8

days after hatching. Stages with significant differences between males and females are marked with an asterisk and bolded (Benjamini Hochberg adjusted p value < 0.05; Table 2). The orange arrow (B) indicates stages where differences in germ counts have been observed between males and females.

822 **Tables**

823 Table 1. Sequence conservation of the threespine *amha* to threespine *amhy* and ninespine *amh.*

Threespine *amha* and threespine *amhy*											
	Exon 1	Exon 2	Exon 3	Exon 4	Exon 5	Exon 6	Exon 7	CDS	Introns	2kb Upstream	2kb Downstream
Sequence identity	0.760	0.682	0.812	0.866	0.790	0.846	0.742	0.780	0.286	0.365	0.376
dN/dS	0.583	0.362	0.512	0.803	0.651	0.373	0.723	0.534	-	-	-
Threespine *amha* and ninespine *amh*											
	Exon 1	Exon 2	Exon 3	Exon 4	Exon 5	Exon 6	Exon 7	CDS	Introns	2kb Upstream	2kb Downstream
Sequence identity	0.791	0.769	0.890	0.920	0.870	0.905	0.936	0.879	0.668	0.595	0.660
dN/dS	0.597	0.425	1.003	0.441	0.266	0.565	0.278	0.467	-	-	-

824

825 Table 2. Benjamini Hochberg adjusted P values for differential expression between males and

826 females.

gene	gene id	stage 17	stage 20	stage 23	0 dah	4 dah	8 dah
amha	amh	1	1	0.679	1	1	1
amhrII	LOC120835457	0.952	1	0.322	1	0.509	**0.0280**
ddx4	ddx4	1	1	1	1	1	**0.00193**
piwil1	piwil1	1	1	1	1	1	**0.00403**
hsd17b1	hsd17b1	1	1	1	0.8681	1	**0.0238**
foxl2a	foxl2a	0.788	1	1	1	1	1
cyp19a1a	LOC120811580	0.662	1	1	1	1	1
dmrt1	dmrt1	1	1	1	1	1	1
sox9b	LOC120827768	0.930	1	1	1	1	1
gsdf	gsdf	1	1	0.467	1	1	1
nr5a1	nr5a1a	1	1	1	1	1	0.983

827

828 Table 3. Phenotypes of mutant stickleback from this study

Genotype	**N**	**Male (%)**	**Female (%)**
F0 XY *amhy* crispants	17	9 (53%)	8 (47%)
F1 XY *amhy*-KO	16	0 (0%)	16 (100%)
F0 XX *Tg(-5amhy2.5,Xla.Ef1a:EGFP)*	16	16 (100%)	0 (0%)
F0 XX *Tg(Xla.Ef1a:EGFP)*	10	0 (0%)	10 (100%)

829

Supplemental figures and tables

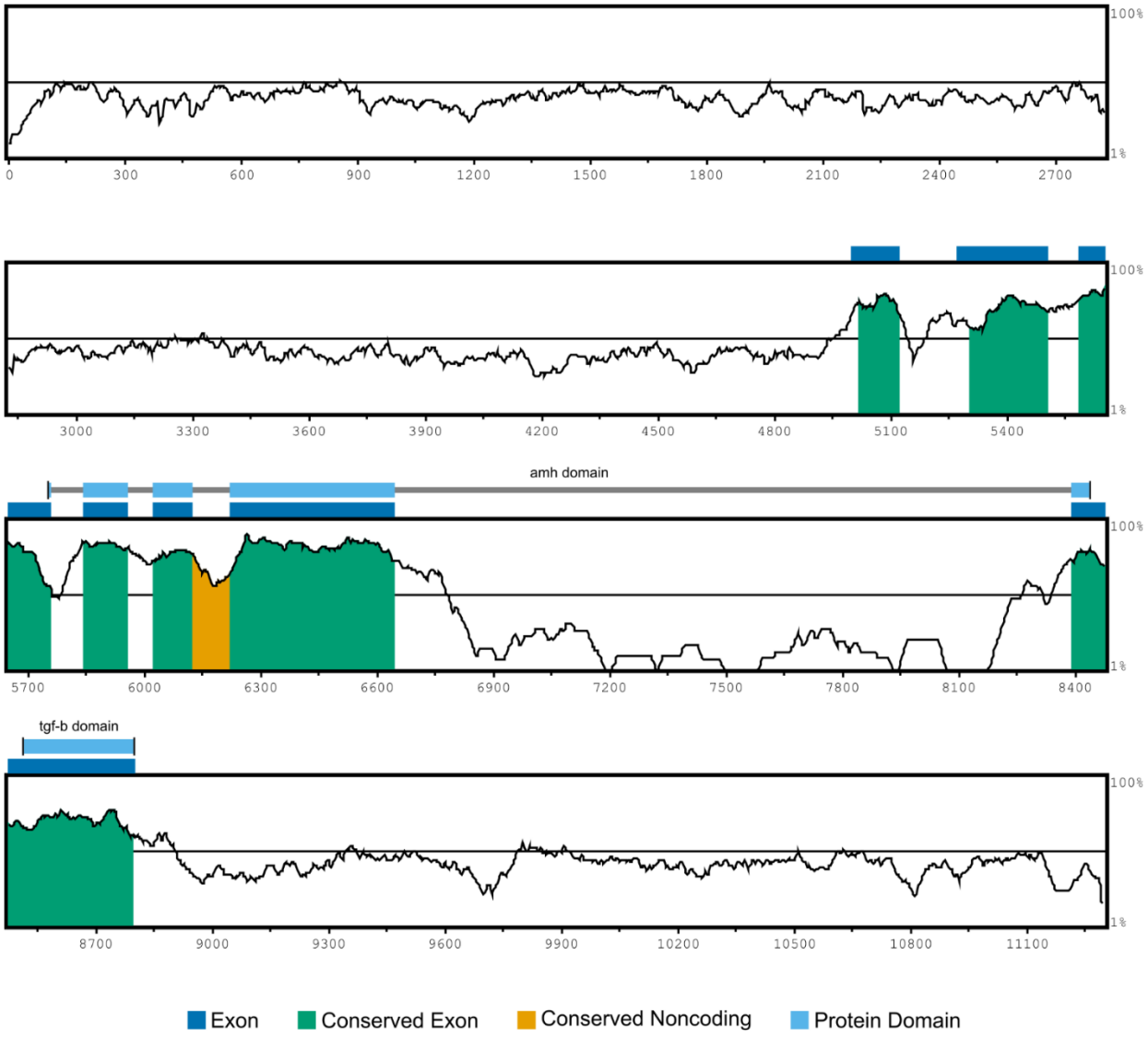

Fig S1. Sequence conservation of the *amhy* transgene region with autosomal *amha*. Vistaplot showing conserved sequence identity of *amhy* to *amha* with sequence identity on the Y axis and base pair position of *amhy* on the x axis. Exon positions are indicated in dark blue, and the amh domain and TGF-β domain are indicated in light blue above the graph. Conserved sequences share 70% sequence identity in a 100 bp window.

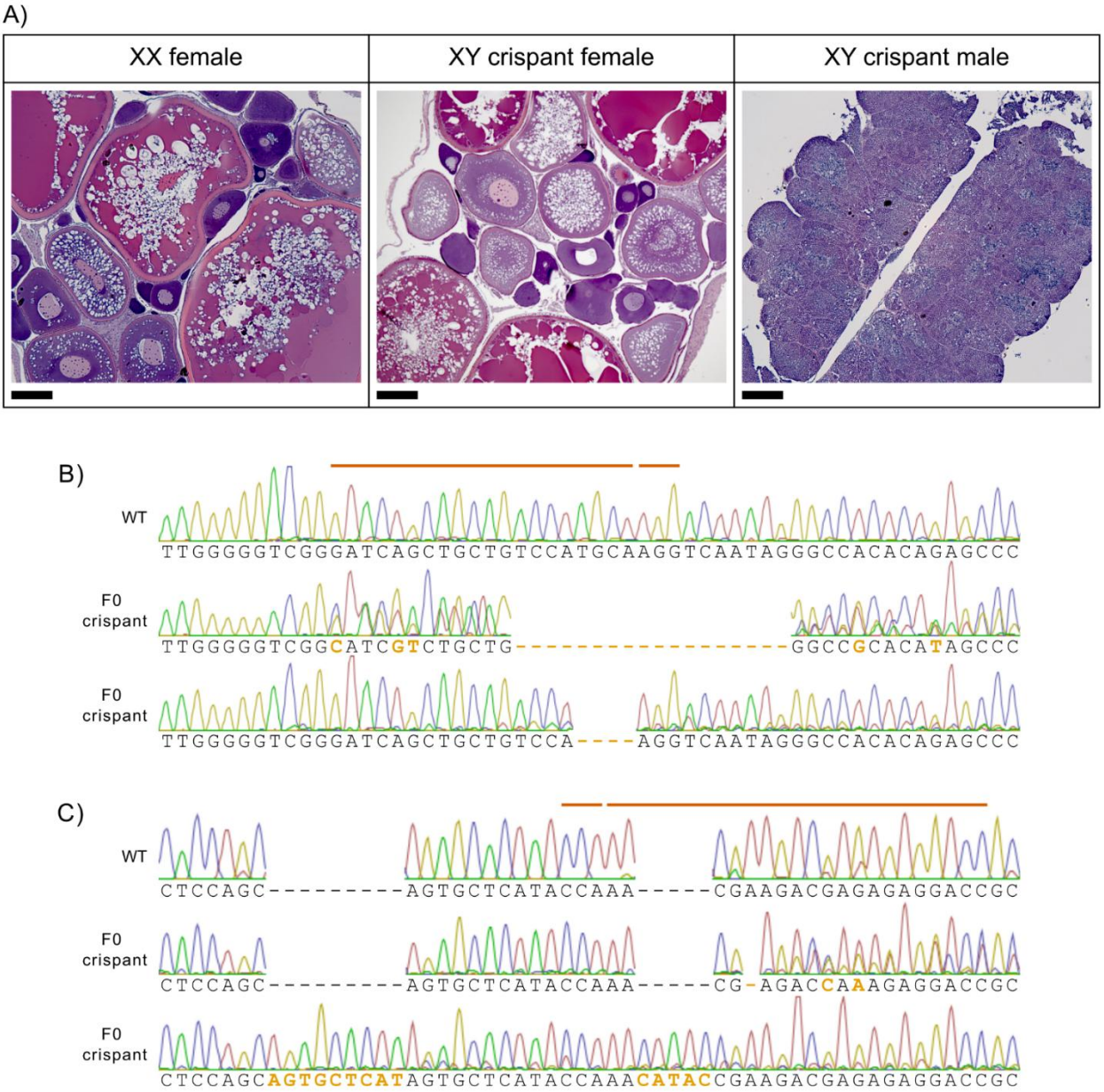

Fig S2. F0 *amhy* crispants show genetic mosaicism and variable sex reversal
A) XY crispants developed as females with ovaries or males with testes. Sanger sequencing of exon 1 (B) and exon 3 (C) show various mutations relative to wildtype. Discordant chromatograms in crispants are indicative of mosaic mutations. Mutations are bolded in orange. CRISPR target site and PAM sequence are indicated by orange lines above wildtype reference sequence.

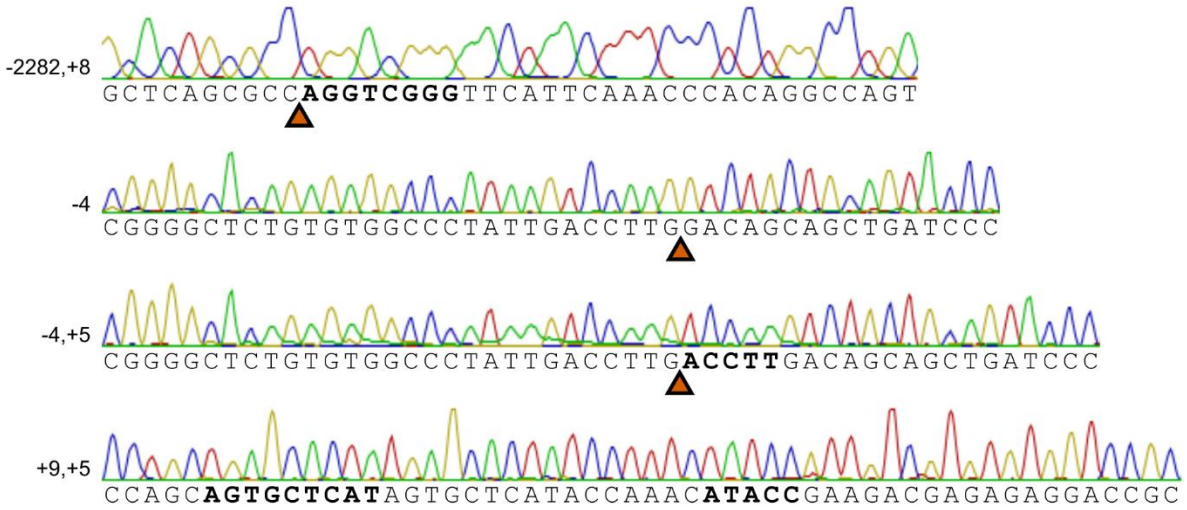

Fig S3. Sanger sequencing of four F1 *amhy* mutant alleles.
Inserted base pairs are bolded. Locations of deletions are indicated with red arrowheads.

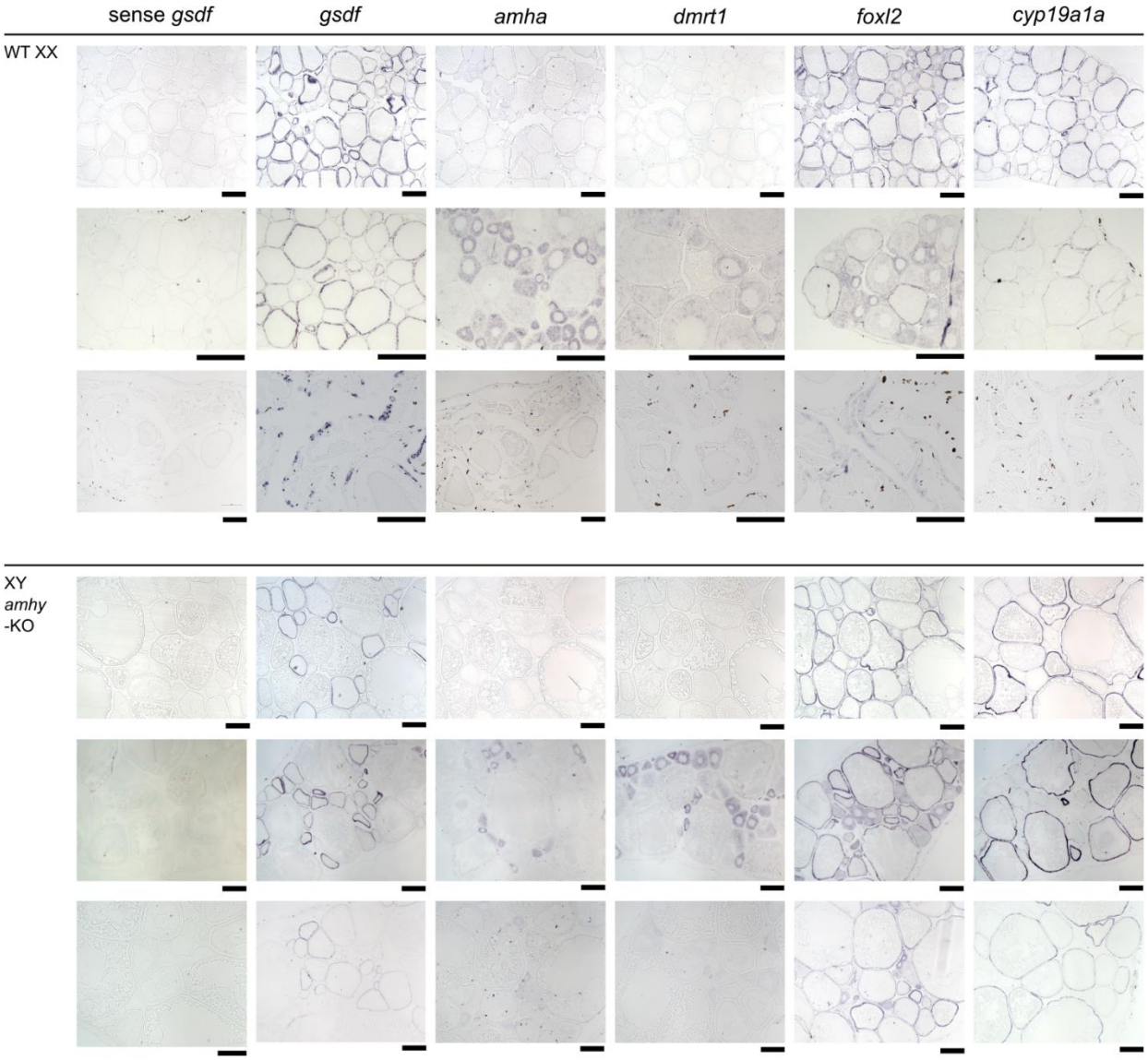

Fig S4. Expression of gonadal genes in wildtype and sex reversed ovaries

In situ hybridization of gonadal genes in three biological replicates for wildtype XX ovaries and XY *amhy*-KO ovaries. Scale bars = 200 μm.

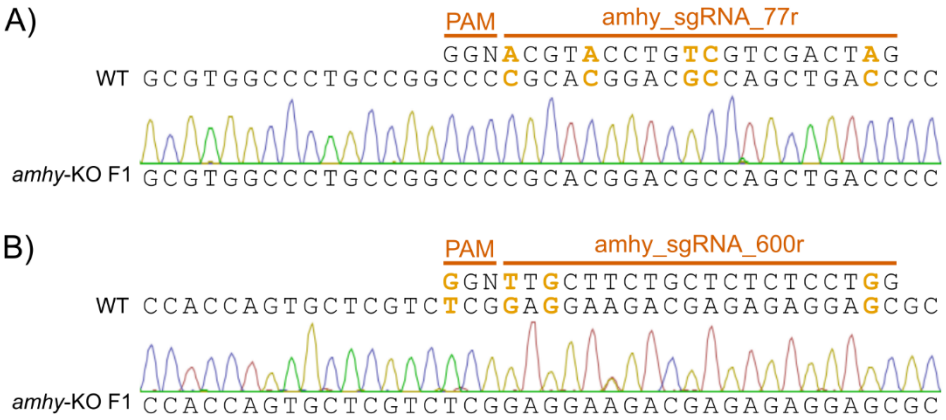

Fig S5. CRISPR/Cas9 sgRNAs for *amhy* have multiple mismatches to their homologous site in *amha*.

PAM and sgRNA sequences are shown above the reference sequence. Mismatched nucleotides are bolded in orange text. Sanger sequencing of sex reversed XY F1 *amhy*-KO fish showed no off-target mutations in *amha* in exon 1 (A) or exon 3 (B).

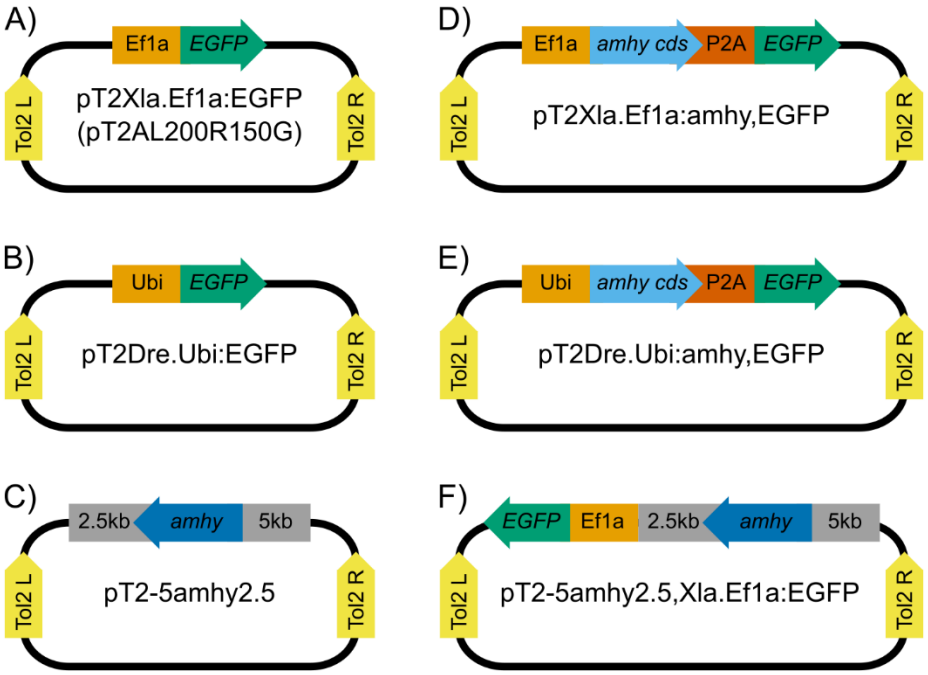

Fig S6. Plasmid maps of transgenes constructed in this study.

Transgenes used the *X. laevis* Ef1a promoter (A and D), *D. rerio* Ubi promoter (B and E), or endogenous *amhy* promoter (C and F). Control transgenes express only EGFP (A and B). Other transgenes contain the *amhy* coding sequence (D and E) or the full *amhy* sequence including introns (C and F). To screen for transgene integration, *amhy* transgenes include an EGFP joined to *amhy* with a P2A self-cleaving peptide (D and E) or separate EGFP cassette (F). All transgenes are flanked by Tol2 transposon arms to facilitate transgene integration.

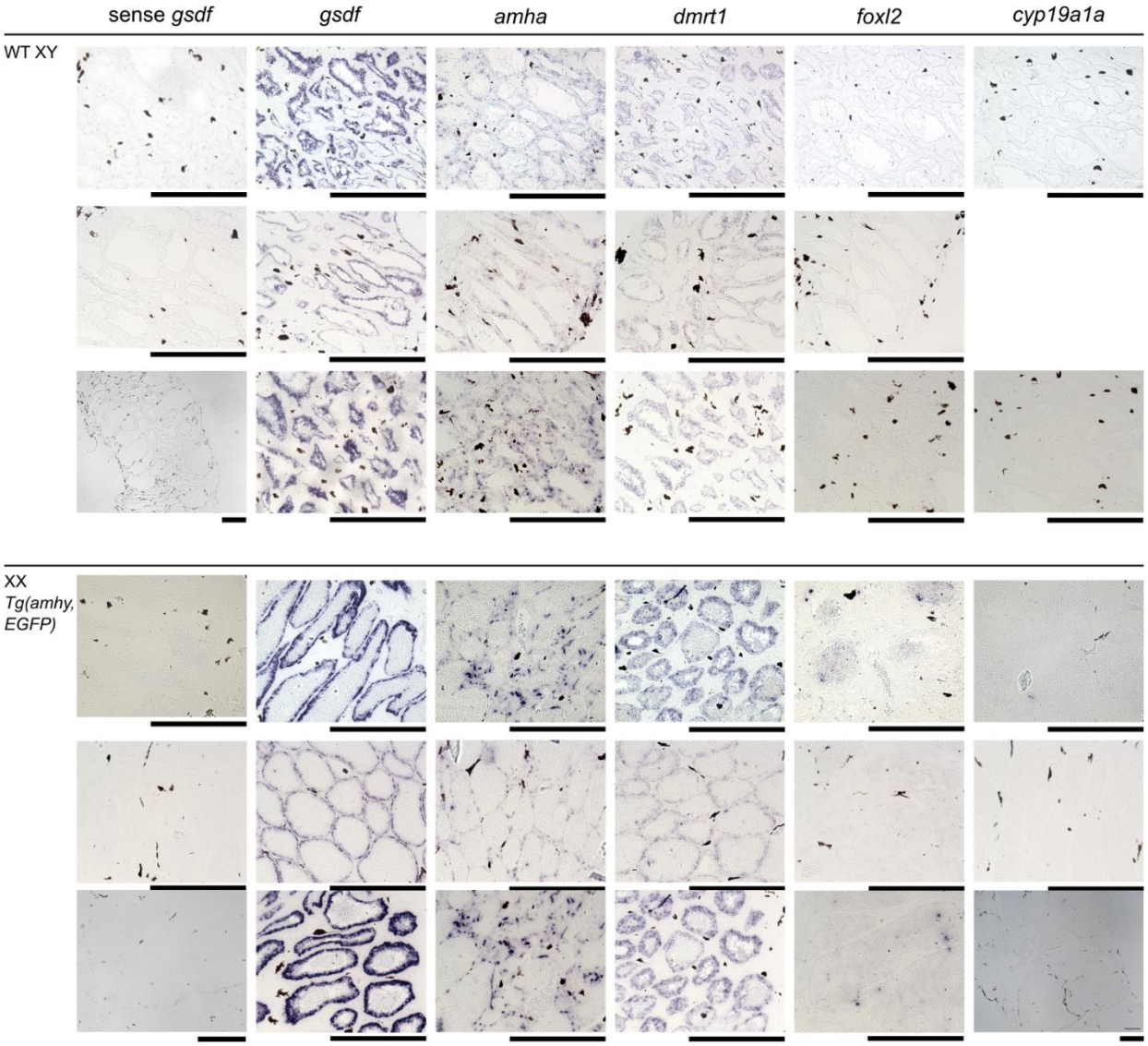

Fig S7. Expression of gonadal genes in wildtype and sex reversed testes.
In situ hybridization of gonadal genes in three biological replicates for wildtype XY testes and XX *Tg(amhy,EGFP)* testes. For one wildtype replicate, the tissue was lost during staining for *cyp19a1a*. Scale bars = 200 µm.

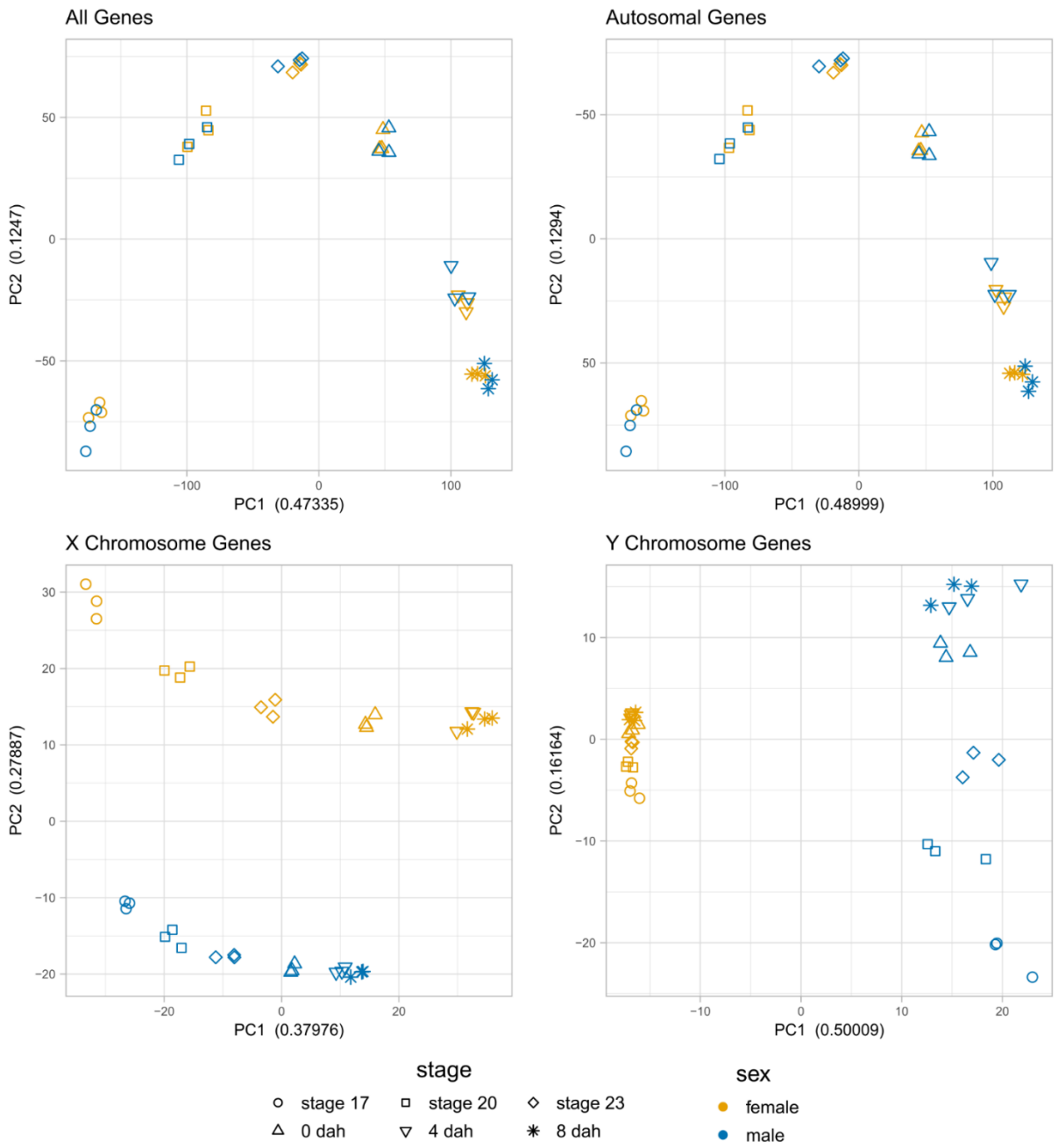

Fig S8. PCA plots of normalized gene expression counts.
Principal components 1 and 2 with the Proportion of Variance Explained on the X and Y axes, respectively. When analyzing all genes or autosomal genes only, samples group by developmental stage and not sex. X chromosome genes show separation by both stage and sex. Y chromosome genes group primarily by sex with male samples separate by developmental stage.

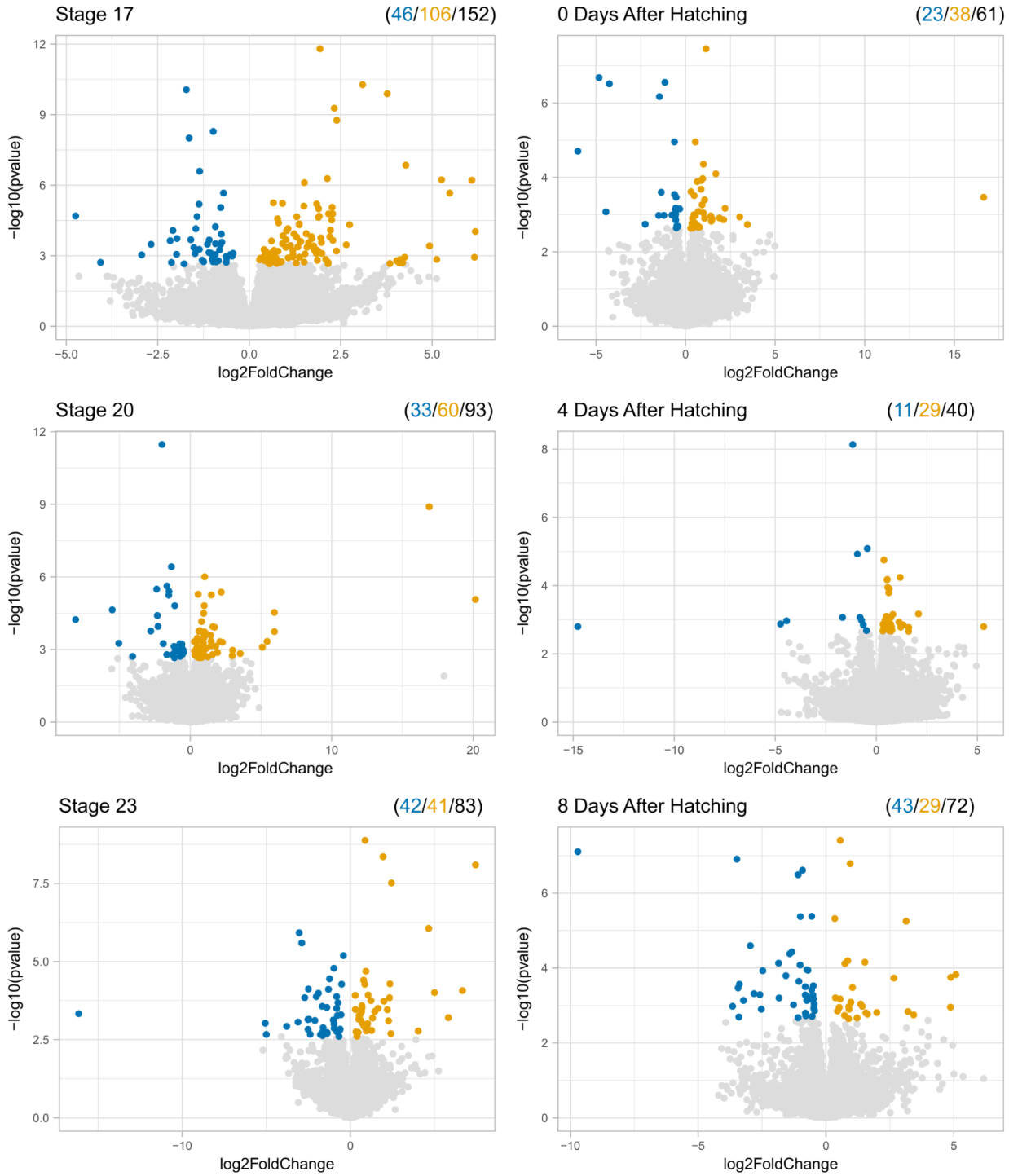

Fig S9. Volcano plots of female to male differential expression by stage. Positive log2 Fold Change values indicate higher expression in females, and negative values indicate higher expression in males. Significant genes (adjusted $p < 0.05$) are shaded. The number of male biased, female biased, and total differentially expressed genes are shown above each plot.

Table S1. Viability and Hatching rates of crosses from F1 XY *amhy*-KO females with wildtype XY males

Fish	Cross number	Clutch Size	Viable	Hatched	Viable:total	Hatched:total	Hatched:viable
A	1	43	1	1	0.0233	0.0233	1.0000
B	1	51	2	0	0.0392	0.0000	0.0000
C	1	63	4	2	0.0635	0.0317	0.5000
C	2	99	24	21	0.2424	0.2121	0.8750
C	3	81	11	6	0.1358	0.0741	0.5455
C	4	100	78	54	0.7800	0.5400	0.6923
C	5	89	70	46	0.7865	0.5169	0.6571

Table S2. Viability and Hatching rates of crosses from F2 XX or XY *amhy*-KO females a wildtype XY male

Genotype	Clutch Size	Viable	Hatched	Viable:total	Hatched:total	Hatched:viable
XX	57	57	57	1.0000	1.0000	1.0000
XX	112	105	34	0.9375	0.3036	0.3238
XX	56	55	55	0.9821	0.9821	1.0000
XX	136	90	47	0.6618	0.3456	0.5222
XX	94	94	79	1.0000	0.8404	0.8404
XY	84	6	2	0.0714	0.0238	0.3333
XY	65	0	0	0.0000	0.0000	NA
XY	98	0	0	0.0000	0.0000	NA
XY	22	0	0	0.0000	0.0000	NA
XY	72	6	4	0.0833	0.0556	0.6667
XY	92	0	0	0.0000	0.0000	NA
Total XX	455	401	272	0.8813	0.5978	0.6783
Total XY	433	12	6	0.0277	0.0139	0.5000

Table S3. Combined *amha* and *amhy* expression show no significant difference between males and females

stage	stage 17		stage 20		stage 23		0 dah		4 dah		8 dah	
sex	female	male	female	male	female	male	female	male	female	male	female	male
amha normalized counts	24.2	31.0	32.5	62.5	142.8	98.1	250.9	248.8	314.6	408.4	348.0	350.2
	35.3	13.2	48.5	37.4	125.2	57.8	288.3	286.2	395.5	286.7	407.7	493.6
	27.5	28.4	54.0	33.1	98.0	109.8	283.8	331.6	318.2	364.8	525.1	431.9
Mean	29.0	24.2	45.0	44.3	122.0	88.6	274.3	288.9	342.8	353.3	426.9	425.2
SD	5.7	9.6	11.2	15.9	22.6	27.3	20.4	41.5	45.7	61.7	90.1	71.9
amhy normalized counts	0	9.4	1.0	3.8	0	14.5	0.9	22.5	0	40.8	0	13.5
	0	10.2	0	4.7	0	13.8	0	20.9	0	20.5	0	32.9
	0	5.7	0	5.2	0	13.0	2.9	8.7	0	16.3	0	9.4
Mean	0	8.4	0.3	4.5	0	13.8	1.3	17.4	0	25.9	0	18.6
sd	0	2.4	0.6	0.7	0	0.8	1.5	7.5	0	13.1	0	12.6
length adjusted *amhy* counts	0	9.38	1.01	3.79	0	14.50	0.85	22.50	0	40.84	0	13.54
	0	10.18	0	4.68	0	13.79	0	20.94	0	20.48	0	32.90
	0	5.68	0	5.17	0	12.96	2.93	8.73	0	16.27	0	9.39
Mean	0	8.42	0.34	4.55	0	13.75	1.26	17.39	0	25.86	0	18.61
SD	0	2.40	0.59	0.70	0	0.77	1.50	7.54	0	13.14	0	12.55
amha + adj. *amhy* normalized counts	24.21	45.59	34.06	68.43	142.76	120.73	252.26	283.91	314.60	472.16	348.00	371.36
	35.34	29.13	48.55	44.72	125.18	79.29	288.27	318.92	395.50	318.66	407.67	544.90
	27.52	37.28	54.01	41.15	97.97	130.05	288.35	345.21	318.15	390.16	525.11	446.56
Mean	29.02	37.33	45.54	51.44	121.97	110.02	276.29	316.01	342.75	393.66	426.93	454.27
SD	5.71	8.23	10.31	14.82	22.57	27.02	20.81	30.75	45.72	76.81	90.11	87.03
P value	0.4078		0.6054		0.5892		0.1474		0.3913		0.7246	

Length adjusted *amhy* counts were calculated by multiplying *amhy* normalized read counts by transcript length of *amha* (3895 bp) divided by *amhy* (2496 bp). P values show two tailed t test for difference in total *amh* expression between males and females at each stage ($P < 0.05$)

904 Table S4 – PCR primers used in this study

Assay	Forward primer	Reverse primer
XY *idh* genotyping	5'-GGGACGAGCAAGATTTATT-3'	5'-TTATCGTTAGCCAGGAGATGG-3'
Amhy exon 1 genotyping, amhy transgene detection	5'-TTGGTGGGTTGATGCTCTGC-3'	5'-CTATGTGAGAGACTGTGGCGG-3'
amhy exon 3 genotyping	5'-TCAGTTTGGAATCTGCACTGTT-3'	5'-GGATGCAGTGATTTACTGGTGA-3'
amhy 2.3 kb deletion genotyping	5'-CACAGTCCTTCGACTCCTTCG-3'	5'-GAGACCATGGTGACTGGCTC-3'
amha exon 1 genotyping	5'-GGCAGTGAGAAGGGAAGGTG-3'	5'-GGCCTCTGGTGATGGGAATG-3'
amha exon 3 genotyping	5'-CAGCCGGAGTCAGTTTGGAA-3'	5'-TCATGCATCGTCGACTGGAG-3'
EGFP transgene detection	5'-ATCATGGCCGACAAGCAGAA-3'	5'-AACTCCAGCAGGACCATGTG-3'
Dmrt1 riboprobe cloning	5'-AGCAGCACCGAGAAGCAG-3'	5'-CTCGTTGACGTTGCCCATGA-3'
Gsdf riboprobe cloning	5'-TTTTGTCACGGCGATGCTTC-3'	5'-AGGAAATGACGAGGGTGCTG-3'
Foxl2 riboprobe cloning	5'-GAGAAGGTCCCGGAGAAAGC-3'	5'-GCAGTGCATCATCGAGAGCT-3'
Cyp19a1a riboprobe cloning	5'-CCTTGTTTCTGTCTGGGCCT-3'	5'-TTGAGGAGCAGCAGCATGA-3'
Riboprobe template synthesis	5'-TAATACGACTCACTATAGGG-3'	5'-TAATACGACTCACTATAGGG-3'

905

References

1. Bachtrog D, Mank JE, Peichel CL, Kirkpatrick M, Otto SP, Ashman T-L, et al. Sex Determination: Why So Many Ways of Doing It? PLoS Biol. 2014;12: e1001899. doi:10.1371/journal.pbio.1001899

2. Capel B. Vertebrate sex determination: evolutionary plasticity of a fundamental switch. Nat Rev Genet. 2017;18: 675–689. doi:10.1038/nrg.2017.60

3. Weber C, Capel B. Sex determination without sex chromosomes. Philosophical Transactions of the Royal Society B: Biological Sciences. 2021;376: 20200109. doi:10.1098/rstb.2020.0109

4. Charlesworth D, Charlesworth B, Marais G. Steps in the evolution of heteromorphic sex chromosomes. Heredity. 2005;95: 118–128. doi:10.1038/sj.hdy.6800697

5. Charlesworth B, Charlesworth D. A Model for the Evolution of Dioecy and Gynodioecy. The American Naturalist. 1978;112: 975–997. doi:10.1086/283342

6. Ponnikas S, Sigeman H, Abbott JK, Hansson B. Why Do Sex Chromosomes Stop Recombining? Trends in Genetics. 2018;34: 492–503. doi:10.1016/j.tig.2018.04.001

7. Pan Q, Kay T, Depincé A, Adolfi M, Schartl M, Guiguen Y, et al. Evolution of master sex determiners: TGF-β signalling pathways at regulatory crossroads. Philosophical Transactions of the Royal Society B: Biological Sciences. 2021;376: 20200091. doi:10.1098/rstb.2020.0091

8. Takehana Y, Matsuda M, Myosho T, Suster ML, Kawakami K, Shin-I T, et al. Co-option of Sox3 as the male-determining factor on the Y chromosome in the fish Oryzias dancena. Nat Commun. 2014;5: 4157. doi:10.1038/ncomms5157

9. Shan Z, Nanda I, Wang Y, Schmid M, Vortkamp A, Haaf T. Sex-specific expression of an evolutionarily conserved male regulatory gene, DMRT1, in birds. Cytogenetics and Cell Genetics. 2000;89: 252–257. doi:10.1159/000015626

10. Yoshimoto S, Okada E, Umemoto H, Tamura K, Uno Y, Nishida-Umehara C, et al. A W-linked DM-domain gene, DM-W, participates in primary ovary development in Xenopus laevis. Proceedings of the National Academy of Sciences. 2008;105: 2469–2474. doi:10.1073/pnas.0712244105

11. Matsuda M, Nagahama Y, Shinomiya A, Sato T, Matsuda C, Kobayashi T, et al. DMY is a Y-specific DM-domain gene required for male development in the medaka fish. Nature. 2002;417: 559–563. doi:10.1038/nature751

12. Nanda I, Kondo M, Hornung U, Asakawa S, Winkler C, Shimizu A, et al. A duplicated copy of DMRT1 in the sex-determining region of the Y chromosome of the medaka, Oryzias latipes. Proceedings of the National Academy of Sciences. 2002;99: 11778–11783. doi:10.1073/pnas.182314699

13. Hattori RS, Murai Y, Oura M, Masuda S, Majhi SK, Sakamoto T, et al. A Y-linked anti-Mullerian hormone duplication takes over a critical role in sex determination. Proceedings

of the National Academy of Sciences. 2012;109: 2955–2959. doi:10.1073/pnas.1018392109

14. Hattori RS, Somoza GM, Fernandino JI, Colautti DC, Miyoshi K, Gong Z, et al. The Duplicated Y-specific amhy Gene Is Conserved and Linked to Maleness in Silversides of the Genus Odontesthes. Genes. 2019;10: 679. doi:10.3390/genes10090679

15. Hattori RS, Kumazawa K, Nakamoto M, Nakano Y, Yamaguchi T, Kitano T, et al. Y-specific amh allele, amhy, is the master sex-determining gene in Japanese flounder Paralichthys olivaceus. Frontiers in Genetics. 2022;13. Available: https://www.frontiersin.org/articles/10.3389/fgene.2022.1007548

16. Li M, Sun Y, Zhao J, Shi H, Zeng S, Ye K, et al. A Tandem Duplicate of Anti-Müllerian Hormone with a Missense SNP on the Y Chromosome Is Essential for Male Sex Determination in Nile Tilapia, Oreochromis niloticus. Naruse K, editor. PLoS Genet. 2015;11: e1005678. doi:10.1371/journal.pgen.1005678

17. Rondeau EB, Laurie CV, Johnson SC, Koop BF. A PCR assay detects a male-specific duplicated copy of Anti-Müllerian hormone (amh) in the lingcod (Ophiodon elongatus). BMC Research Notes. 2016;9: 230. doi:10.1186/s13104-016-2030-6

18. Bej DK, Miyoshi K, Hattori RS, Strüssmann CA, Yamamoto Y. A Duplicated, Truncated amh Gene Is Involved in Male Sex Determination in an Old World Silverside. G3 Genes|Genomes|Genetics. 2017;7: 2489–2495. doi:10.1534/g3.117.042697

19. Pan Q, Feron R, Yano A, Guyomard R, Jouanno E, Vigouroux E, et al. Identification of the master sex determining gene in Northern pike (Esox lucius) reveals restricted sex chromosome differentiation. PLOS Genetics. 2019;15: e1008013. doi:10.1371/journal.pgen.1008013

20. Peichel CL, McCann SR, Ross JA, Naftaly AFS, Urton JR, Cech JN, et al. Assembly of the threespine stickleback Y chromosome reveals convergent signatures of sex chromosome evolution. Genome Biol. 2020;21: 177. doi:10.1186/s13059-020-02097-x

21. Song W, Xie Y, Sun M, Li X, Fitzpatrick CK, Vaux F, et al. A duplicated amh is the master sex-determining gene for Sebastes rockfish in the Northwest Pacific. Open Biology. 2021;11: 210063. doi:10.1098/rsob.210063

22. Jeffries DL, Mee JA, Peichel CL. Identification of a candidate sex determination gene in Culaea inconstans suggests convergent recruitment of an Amh duplicate in two lineages of stickleback. Journal of Evolutionary Biology. 2022;n/a. doi:10.1111/jeb.14034

23. Zhao H, Li J, Xiao Z, Xiao Y. Dose-dependent role of AMH and AMHR2 signaling in male differentiation and regulation of sex determination in Spotted knifejaw (Oplegnathus punctatus) with X1X1X2X2/X1X2Y chromosome system. Cell Communication and Signaling. 2025;23: 59. doi:10.1186/s12964-025-02038-w

24. Wang T, Gong G, Li Z, Niu J-S, Du W-X, Wang Z-W, et al. Genomic Anatomy of Homozygous XX Females and YY Males Reveals Early Evolutionary Trajectory of Sex-determining Gene and Sex Chromosomes in Silurus Fishes. Molecular Biology and Evolution. 2024;41: msae169. doi:10.1093/molbev/msae169

25. Cortez D, Marin R, Toledo-Flores D, Froidevaux L, Liechti A, Waters PD, et al. Origins and functional evolution of Y chromosomes across mammals. Nature. 2014;508: 488–493. doi:10.1038/nature13151

26. Mullen RD, Ontiveros AE, Moses MM, Behringer RR. AMH and AMHR2 mutations: A spectrum of reproductive phenotypes across vertebrate species. Developmental Biology. 2019;455: 1–9. doi:10.1016/j.ydbio.2019.07.006

27. Howard JA, Hart KN, Thompson TB. Molecular Mechanisms of AMH Signaling. Frontiers in Endocrinology. 2022;13. Available: https://www.frontiersin.org/articles/10.3389/fendo.2022.927824

28. Baarends WM, Helmond MJL van, Post M, Schoot PJCM van der, Hoogerbrugge JW, Winter JP de, et al. A novel member of the transmembrane serine/threonine kinase receptor family is specifically expressed in the gonads and in mesenchymal cells adjacent to the müllerian duct. Development. 1994;120: 189–197. doi:10.1242/dev.120.1.189

29. Josso N, di Clemente N, Gouédard L. Anti-Müllerian hormone and its receptors. Molecular and Cellular Endocrinology. 2001;179: 25–32. doi:10.1016/S0303-7207(01)00467-1

30. Mishina Y, Whitworth DJ, Racine C, Behringer RR. High Specificity of Müllerian-Inhibiting Substance Signaling in Vivo*. Endocrinology. 1999;140: 2084–2088. doi:10.1210/endo.140.5.6705

31. Jost A. The Age Factor in the Castration of Male Rabbit Fetuses. Proceedings of the Society for Experimental Biology and Medicine. 1947;66: 302–303. doi:10.3181/00379727-66-16071

32. Morinaga C, Saito D, Nakamura S, Sasaki T, Asakawa S, Shimizu N, et al. The hotei mutation of medaka in the anti-Müllerian hormone receptor causes the dysregulation of germ cell and sexual development. PNAS. 2007;104: 9691–9696. doi:10.1073/pnas.0611379104

33. Pfennig F, Standke A, Gutzeit HO. The role of Amh signaling in teleost fish – Multiple functions not restricted to the gonads. General and Comparative Endocrinology. 2015;223: 87–107. doi:10.1016/j.ygcen.2015.09.025

34. Yan Y-L, Batzel P, Titus T, Sydes J, Desvignes T, BreMiller R, et al. A Hormone That Lost Its Receptor: Anti-Müllerian Hormone (AMH) in Zebrafish Gonad Development and Sex Determination. Genetics. 2019;213: 529–553. doi:10.1534/genetics.119.302365

35. Ross JA, Urton JR, Boland J, Shapiro MD, Peichel CL. Turnover of Sex Chromosomes in the Stickleback Fishes (Gasterosteidae). PLOS Genetics. 2009;5: e1000391. doi:10.1371/journal.pgen.1000391

36. Dixon G, Kitano J, Kirkpatrick M. The Origin of a New Sex Chromosome by Introgression between Two Stickleback Fishes. Molecular Biology and Evolution. 2019;36: 28–38. doi:10.1093/molbev/msy181

37. Natri HM, Merilä J, Shikano T. The evolution of sex determination associated with a chromosomal inversion. Nat Commun. 2019;10: 145. doi:10.1038/s41467-018-08014-y

38. Sardell JM, Josephson MP, Dalziel AC, Peichel CL, Kirkpatrick M. Heterogeneous Histories of Recombination Suppression on Stickleback Sex Chromosomes. Molecular Biology and Evolution. 2021;38: 4403–4418. doi:10.1093/molbev/msab179

39. Peichel CL, Ross JA, Matson CK, Dickson M, Grimwood J, Schmutz J, et al. The Master Sex-Determination Locus in Threespine Sticklebacks Is on a Nascent Y Chromosome. Current Biology. 2004;14: 1416–1424. doi:10.1016/j.cub.2004.08.030

40. Pigott GC, Akel MA, Rogers MGQ, Flanagan ME, Marlette EG, Treaster MJ, et al. Evidence for Variation in the Genetic Basis of Sex Determination in Brook Stickleback (Culaea inconstans). Ecology and Evolution. 2025;15: e70955. doi:10.1002/ece3.70955

41. Erickson PA, Ellis NA, Miller CT. Microinjection for Transgenesis and Genome Editing in Threespine Sticklebacks. J Vis Exp. 2016 [cited 30 Jan 2021]. doi:10.3791/54055

42. Nath S, Shaw DE, White MA. Improved contiguity of the threespine stickleback genome using long-read sequencing. G3 Genes|Genomes|Genetics. 2021;11. doi:10.1093/g3journal/jkab007

43. Aguirre WE, Ellis KE, Kusenda M, Bell MA. Phenotypic variation and sexual dimorphism in anadromous threespine stickleback: implications for postglacial adaptive radiation. Biological Journal of the Linnean Society. 2008;95: 465–478. doi:10.1111/j.1095-8312.2008.01075.x

44. Leinonen T, Cano JM, Merilä J. Genetic basis of sexual dimorphism in the threespine stickleback Gasterosteus aculeatus. Heredity. 2011;106: 218–227. doi:10.1038/hdy.2010.104

45. Kitano J, Mori S, Peichel CL. Sexual Dimorphism in the External Morphology of the Threespine Stickleback (Gasterosteus Aculeatus). Copeia. 2007;2007: 336–349. doi:10.1643/0045-8511(2007)7[336:SDITEM]2.0.CO;2

46. Aguirre WE, Akinpelu O. Sexual dimorphism of head morphology in three-spined stickleback Gasterosteus aculeatus. Journal of Fish Biology. 2010;77: 802–821. doi:10.1111/j.1095-8649.2010.02705.x

47. Toli EA, Noreikiene K, DeFaveri J, Merilä J. Environmental enrichment, sexual dimorphism, and brain size in sticklebacks. Ecology and Evolution. 2017;7: 1691–1698. doi:10.1002/ece3.2717

48. Kotrschal A, Räsänen K, Kristjánsson BK, Senn M, Kolm N. Extreme Sexual Brain Size Dimorphism in Sticklebacks: A Consequence of the Cognitive Challenges of Sex and Parenting? PLOS ONE. 2012;7: e30055. doi:10.1371/journal.pone.0030055

49. McGee MD, Wainwright PC. Sexual dimorphism in the feeding mechanism of threespine stickleback. Journal of Experimental Biology. 2013;216: 835–840. doi:10.1242/jeb.074948

50. Whoriskey FG, FitzGerald GJ. Sex, cannibalism and sticklebacks. Behav Ecol Sociobiol. 1985;18: 15–18. doi:10.1007/BF00299233

51. King AJ, Fürtbauer I, Mamuneas D, James C, Manica A. Sex-Differences and Temporal Consistency in Stickleback Fish Boldness. PLOS ONE. 2013;8: e81116. doi:10.1371/journal.pone.0081116

52. FitzGerald GJ. The Reproductive Behavior of the Stickleback. Scientific American. 1993;268: 80–85.

53. Bell MA, Foster SA. The Evolutionary Biology of the Threespine Stickleback. The Journal of Animal Ecology. 1994;64: 418. doi:10.2307/5902

54. Pressley PH. Parental Effort and the Evolution of Nest-Guarding Tactics in the Threespine Stickleback, Gasterosteus aculeatus L. Evolution. 1981;35: 282–295. doi:10.2307/2407838

55. Bakker TCM, Künzler R, Mazzi D. Condition-related mate choice in sticklebacks. Nature. 1999;401: 234–234. doi:10.1038/45727

56. Milinski M, Bakker TCM. Female sticklebacks use male coloration in mate choice and hence avoid parasitized males. Nature. 1990;344: 330–333. doi:10.1038/344330a0

57. Conte GL, Schluter D. Experimental Confirmation That Body Size Determines Mate Preference via Phenotype Matching in a Stickleback Species Pair. Evolution. 2013;67: 1477–1484. doi:10.1111/evo.12041

58. Andreou D, Eizaguirre C, Boehm T, Milinski M. Mate choice in sticklebacks reveals that immunogenes can drive ecological speciation. Behavioral Ecology. 2017;28: 953–961. doi:10.1093/beheco/arx074

59. Milinski M. The function of mate choice in sticklebacks: optimizing Mhc genetics. Journal of Fish Biology. 2003;63: 1–16. doi:10.1111/j.1095-8649.2003.00215.x

60. Flamarique IN, Bergstrom C, Cheng CL, Reimchen TE. Role of the iridescent eye in stickleback female mate choice. Journal of Experimental Biology. 2013;216: 2806–2812. doi:10.1242/jeb.084889

61. Barker TCM, Milinski M. The advantages of being red: Sexual selection in the stickleback. Marine & Freshwater Behaviour & Phy. 1993 [cited 21 Apr 2025]. doi:10.1080/10236249309378870

62. Candolin U. Reproduction under predation risk and the trade–off between current and future reproduction in the threespine stickleback. Proceedings of the Royal Society of London Series B: Biological Sciences. 1998;265: 1171–1175. doi:10.1098/rspb.1998.0415

63. Johnson S, Candolin U. Predation cost of a sexual signal in the threespine stickleback. Behavioral Ecology. 2017;28: 1160–1165. doi:10.1093/beheco/arx080

1095 64. Borg B, Mayer I, Hoffmann E, Österman A. 11-ketotestosterone is not responsible for the
1096 entire testicular effect on male reproductive behaviour in the threespine stickleback.
1097 Behav. 2008;145: 509–525. doi:10.1163/156853908792451548

1098 65. Shibata Y, Paul-Prasanth B, Suzuki A, Usami T, Nakamoto M, Matsuda M, et al.
1099 Expression of gonadal soma derived factor (GSDF) is spatially and temporally correlated
1100 with early testicular differentiation in medaka. Gene Expression Patterns. 2010;10: 283–
1101 289. doi:10.1016/j.gep.2010.06.005

1102 66. Guo Y, Cheng H, Huang X, Gao S, Yu H, Zhou R. Gene structure, multiple alternative
1103 splicing, and expression in gonads of zebrafish *Dmrt1*. Biochemical and Biophysical
1104 Research Communications. 2005;330: 950–957. doi:10.1016/j.bbrc.2005.03.066

1105 67. von Hofsten J, Larsson A, Olsson P e. Novel steroidogenic factor-1 homolog (ff1d) is
1106 coexpressed with anti-Mullerian hormone (AMH) in zebrafish. Developmental Dynamics.
1107 2005;233: 595–604. doi:10.1002/dvdy.20335

1108 68. Johnsen H, Seppola M, Torgersen JS, Delghandi M, Andersen Ø. Sexually dimorphic
1109 expression of *dmrt1* in immature and mature Atlantic cod (*Gadus morhua* L.).
1110 Comparative Biochemistry and Physiology Part B: Biochemistry and Molecular Biology.
1111 2010;156: 197–205. doi:10.1016/j.cbpb.2010.03.009

1112 69. von Schalburg KR, Gowen BE, Rondeau EB, Johnson NW, Minkley DR, Leong JS, et al.
1113 Sex-specific expression, synthesis and localization of aromatase regulators in one-year-
1114 old Atlantic salmon ovaries and testes. Comparative Biochemistry and Physiology Part B:
1115 Biochemistry and Molecular Biology. 2013;164: 236–246. doi:10.1016/j.cbpb.2013.01.004

1116 70. Kossack ME, Draper BW. Genetic regulation of sex determination and maintenance in
1117 zebrafish (Danio rerio). Curr Top Dev Biol. 2019;134: 119–149.
1118 doi:10.1016/bs.ctdb.2019.02.004

1119 71. Urasaki A, Morvan G, Kawakami K. Functional Dissection of the Tol2 Transposable
1120 Element Identified the Minimal cis-Sequence and a Highly Repetitive Sequence in the
1121 Subterminal Region Essential for Transposition. Genetics. 2006;174: 639–649.
1122 doi:10.1534/genetics.106.060244

1123 72. Kawakami K, Takeda H, Kawakami N, Kobayashi M, Matsuda N, Mishina M. A
1124 Transposon-Mediated Gene Trap Approach Identifies Developmentally Regulated Genes
1125 in Zebrafish. Developmental Cell. 2004;7: 133–144. doi:10.1016/j.devcel.2004.06.005

1126 73. Kim JH, Lee S-R, Li L-H, Park H-J, Park J-H, Lee KY, et al. High Cleavage Efficiency of a
1127 2A Peptide Derived from Porcine Teschovirus-1 in Human Cell Lines, Zebrafish and Mice.
1128 PLOS ONE. 2011;6: e18556. doi:10.1371/journal.pone.0018556

1129 74. Liu Z, Chen O, Wall JBJ, Zheng M, Zhou Y, Wang L, et al. Systematic comparison of 2A
1130 peptides for cloning multi-genes in a polycistronic vector. Scientific Reports. 2017;7:
1131 2193. doi:10.1038/s41598-017-02460-2

1132 75. Mosimann C, Kaufman CK, Li P, Pugach EK, Tamplin OJ, Zon LI. Ubiquitous transgene
1133 expression and Cre-based recombination driven by the ubiquitin promoter in zebrafish.
1134 Development. 2011;138: 169–177. doi:10.1242/dev.059345

76. Ueda Y, Mizuno N, Araki M. Transgenic Xenopus laevis with the ef1-α promoter as an experimental tool for amphibian retinal regeneration study. genesis. 2012;50: 642–650. doi:10.1002/dvg.22024

77. Wootton RJ. A Functional Biology of Sticklebacks. 1st ed. University of California Press; 1984. doi:10.2307/jj.8306147

78. Varadharajan S, Rastas P, Löytynoja A, Matschiner M, Calboli FCF, Guo B, et al. A High-Quality Assembly of the Nine-Spined Stickleback (Pungitius pungitius) Genome. Genome Biology and Evolution. 2019;11: 3291–3308. doi:10.1093/gbe/evz240

79. Bachtrog D. Y-chromosome evolution: emerging insights into processes of Y-chromosome degeneration. Nat Rev Genet. 2013;14: 113–124. doi:10.1038/nrg3366

80. Swarup H. Stages in the Development of the Stickleback Gasterosteus aculeatus (L.). Development. 1958;6: 373–383.

81. Lewis ZR, McClellan MC, Postlethwait JH, Cresko WA, Kaplan RH. Female-specific increase in primordial germ cells marks sex differentiation in threespine stickleback (*Gasterosteus aculeatus*). J Morphol. 2008;269: 909–921. doi:10.1002/jmor.10608

82. Shi D-L. Interplay of RNA-binding proteins controls germ cell development in zebrafish. Journal of Genetics and Genomics. 2024;51: 889–899. doi:10.1016/j.jgg.2024.06.020

83. Planells B, Gómez-Redondo I, Pericuesta E, Lonergan P, Gutiérrez-Adán A. Differential isoform expression and alternative splicing in sex determination in mice. BMC Genomics. 2019;20: 202. doi:10.1186/s12864-019-5572-x

84. Mindnich R, Deluca D, Adamski J. Identification and characterization of 17β-hydroxysteroid dehydrogenases in the zebrafish, *Danio rerio*. Molecular and Cellular Endocrinology. 2004;215: 19–30. doi:10.1016/j.mce.2003.11.010

85. Koyama T, Nakamoto M, Morishima K, Yamashita R, Yamashita T, Sasaki K, et al. A SNP in a Steroidogenic Enzyme Is Associated with Phenotypic Sex in Seriola Fishes. Current Biology. 2019;29: 1901-1909.e8. doi:10.1016/j.cub.2019.04.069

86. Lasalle A, Benech-Correa G, Brunet FG, Vizziano-Cantonnet D. hsd17b1 is a key gene for ovarian differentiation of the Siberian sturgeon. Molecular Reproduction and Development. 2024;91: e23729. doi:10.1002/mrd.23729

87. Desaulniers AT, Cederberg RA, Lents CA, White BR. Expression and Role of Gonadotropin-Releasing Hormone 2 and Its Receptor in Mammals. Front Endocrinol. 2017;8. doi:10.3389/fendo.2017.00269

88. Sarraj MA, Sarraj ,Mai A., Chua ,Hui Kheng, Sarraj ,Mai A., Chua ,Hui Kheng, Umbers ,Alexandra, et al. Differential expression of TGFBR3 (betaglycan) in mouse ovary and testis during gonadogenesis. Growth Factors. 2007;25: 334–345. doi:10.1080/08977190701833619

1171 89. Wickramasinghe D, Becker S, Ernst MK, Resnick JL, Centanni JM, Tessarollo L, et al.
1172 Two CDC25 homologues are differentially expressed during mouse development.
1173 Development. 1995;121: 2047–2056. doi:10.1242/dev.121.7.2047

1174 90. Namgoong S, Kim N-H. Meiotic spindle formation in mammalian oocytes: implications for
1175 human infertility†. Biology of Reproduction. 2018;98: 153–161. doi:10.1093/biolre/iox145

1176 91. Strüssmann CA, Saito T, Usui M, Yamada H, Takashima F. Thermal thresholds and critical
1177 period of thermolabile sex determination in two atherinid fishes, Odontesthes bonariensis
1178 and Patagonina hatcheri. Journal of Experimental Zoology. 1997;278: 167–177.
1179 doi:10.1002/(SICI)1097-010X(19970615)278:3<167::AID-JEZ6>3.0.CO;2-M

1180 92. Baroiller JF, D'Cotta H, Bezault E, Wessels S, Hoerstgen-Schwark G. Tilapia sex
1181 determination: Where temperature and genetics meet. Comparative Biochemistry and
1182 Physiology Part A: Molecular & Integrative Physiology. 2009;153: 30–38.
1183 doi:10.1016/j.cbpa.2008.11.018

1184 93. Sun P, You F, Ma D, Li J, Zhang P. Sex steroid changes during temperature-induced
1185 gonadal differentiation in (Temminck & Schegel, 1846). Journal of Applied Ichthyology.
1186 2013;29: 886–890. doi:10.1111/jai.12128

1187 94. Borg B, van den Hurk R. Oocytes in the Testes of the Three-Spined Stickleback,
1188 Gasterosteus aculeatus. Copeia. 1983;1983: 259–261. doi:10.2307/1444727

1189 95. Gercken J, Sordyl H. Intersex in feral marine and freshwater fish from northeastern
1190 Germany. Marine Environmental Research. 2002;54: 651–655. doi:10.1016/S0141-
1191 1136(02)00156-3

1192 96. Aharon D, Marlow FL. Sexual determination in zebrafish. Cell Mol Life Sci. 2021;79: 8.
1193 doi:10.1007/s00018-021-04066-4

1194 97. Slanchev K, Stebler J, de la Cueva-Méndez G, Raz E. Development without germ cells:
1195 The role of the germ line in zebrafish sex differentiation. Proceedings of the National
1196 Academy of Sciences. 2005;102: 4074–4079. doi:10.1073/pnas.0407475102

1197 98. Tzung K-W, Goto R, Saju JM, Sreenivasan R, Saito T, Arai K, et al. Early Depletion of
1198 Primordial Germ Cells in Zebrafish Promotes Testis Formation. Stem Cell Reports.
1199 2015;4: 61–73. doi:10.1016/j.stemcr.2014.10.011

1200 99. Schartl M. A comparative view on sex determination in medaka. Mechanisms of
1201 Development. 2004;121: 639–645. doi:10.1016/j.mod.2004.03.001

1202 100. Kurokawa H, Saito D, Nakamura S, Katoh-Fukui Y, Ohta K, Baba T, et al. Germ cells are
1203 essential for sexual dimorphism in the medaka gonad. Proceedings of the National
1204 Academy of Sciences. 2007;104: 16958–16963. doi:10.1073/pnas.0609932104

1205 101. Nakamura S, Watakabe I, Nishimura T, Picard J-Y, Toyoda A, Taniguchi Y, et al.
1206 Hyperproliferation of mitotically active germ cells due to defective anti-Müllerian hormone
1207 signaling mediates sex reversal in medaka. Development. 2012;139: 2283–2287.
1208 doi:10.1242/dev.076307

1209 102. Tezak B, Straková B, Fullard DJ, Dupont S, McKey J, Weber C, et al. Higher
1210 temperatures directly increase germ cell number, promoting feminization of red-eared
1211 slider turtles. Current Biology. 2023;0. doi:10.1016/j.cub.2023.06.008

1212 103. Lyet L, Louis F, Forest MG, Josso N, Behringer RR, Vigier B. Ontogeny of Reproductive
1213 Abnormalities Induced by Deregulation of Anti-Müllerian Hormone Expression in
1214 Transgenic Mice. Biology of Reproduction. 1995;52: 444–454.
1215 doi:10.1095/biolreprod52.2.444

1216 104. Han Y, Zhao M, Wang L, Yu Z, Wang J, Yu Q, et al. Overexpression of Anti-müllerian
1217 Hormone Gene in vivo Affects Gonad Sex Differentiation in Undifferentiated Orange-
1218 Spotted Groupers (Epinephelus coioides). Front Endocrinol. 2019;0.
1219 doi:10.3389/fendo.2019.00210

1220 105. Rehman Z ur, Worku T, Davis JS, Talpur HS, Bhattarai D, Kadariya I, et al. Role and
1221 mechanism of AMH in the regulation of Sertoli cells in mice. The Journal of Steroid
1222 Biochemistry and Molecular Biology. 2017;174: 133–140.
1223 doi:10.1016/j.jsbmb.2017.08.011

1224 106. Rodriguez KF, Brown PR, Amato CM, Nicol B, Liu C-F, Xu X, et al. Somatic cell fate
1225 maintenance in mouse fetal testes via autocrine/paracrine action of AMH and activin B.
1226 Nat Commun. 2022;13: 4130. doi:10.1038/s41467-022-31486-y

1227 107. Guiguen Y, Fostier A, Piferrer F, Chang C-F. Ovarian aromatase and estrogens: A pivotal
1228 role for gonadal sex differentiation and sex change in fish. General and Comparative
1229 Endocrinology. 2010;165: 352–366. doi:10.1016/j.ygcen.2009.03.002

1230 108. Li M, Sun L, Wang D. Roles of estrogens in fish sexual plasticity and sex differentiation.
1231 General and Comparative Endocrinology. 2019;277: 9–16.
1232 doi:10.1016/j.ygcen.2018.11.015

1233 109. Liu X, Dai S, Wu J, Wei X, Zhou X, Chen M, et al. Roles of anti-Müllerian hormone and its
1234 duplicates in sex determination and germ cell proliferation of Nile tilapia. Genetics. 2021;
1235 iyab237. doi:10.1093/genetics/iyab237

1236 110. Halm S, Rocha A, Miura T, Prat F, Zanuy S. Anti-Müllerian hormone (*AMH*/AMH) in the
1237 European sea bass: Its gene structure, regulatory elements, and the expression of
1238 alternatively-spliced isoforms. Gene. 2007;388: 148–158. doi:10.1016/j.gene.2006.10.018

1239 111. Liu X, Xiao H, Jie M, Dai S, Wu X, Li M, et al. Amh regulate female folliculogenesis and
1240 fertility in a dose-dependent manner through Amhr2 in Nile tilapia. Molecular and Cellular
1241 Endocrinology. 2020;499: 110593. doi:10.1016/j.mce.2019.110593

1242 112. Wu K, Yue Y, Zhou L, Zhang Z, Shan H, He H, et al. Disrupting Amh and androgen
1243 signaling reveals their distinct roles in zebrafish gonadal differentiation and
1244 gametogenesis. Commun Biol. 2025;8: 1–15. doi:10.1038/s42003-025-07719-3

1245 113. Zhang Z, Wu K, Ren Z, Ge W. Genetic evidence for Amh modulation of gonadotropin
1246 actions to control gonadal homeostasis and gametogenesis in zebrafish and its
1247 noncanonical signaling through Bmpr2a receptor. Development. 2020;147: dev189811.
1248 doi:10.1242/dev.189811

114. Ijiri S, Kaneko H, Kobayashi T, Wang D-S, Sakai F, Paul-Prasanth B, et al. Sexual Dimorphic Expression of Genes in Gonads During Early Differentiation of a Teleost Fish, the Nile Tilapia Oreochromis niloticus1. Biology of Reproduction. 2008;78: 333–341. doi:10.1095/biolreprod.107.064246

115. Czerwinski M, Natarajan A, Barske L, Looger LL, Capel B. A timecourse analysis of systemic and gonadal effects of temperature on sexual development of the red-eared slider turtle Trachemys scripta elegans. Developmental Biology. 2016;420: 166–177. doi:10.1016/j.ydbio.2016.09.018

116. Sánchez-Baizán N, Jarne-Sanz I, Roco ÁS, Schartl M, Piferrer F. Extraordinary variability in gene activation and repression programs during gonadal sex differentiation across vertebrates. Front Cell Dev Biol. 2024;12. doi:10.3389/fcell.2024.1328365

117. Hacker A, Capel B, Goodfellow P, Lovell-Badge R. Expression of Sry, the mouse sex determining gene. Development. 1995;121: 1603–1614. doi:10.1242/dev.121.6.1603

118. Kobayashi T, Nagahama Y. Molecular Aspects of Gonadal Differentiation in a Teleost Fish, the Nile Tilapia. Sexual Development. 2009;3: 108–117. doi:10.1159/000223076

119. Eshel O, Shirak A, Weller JI, Hulata G, Ron M. Linkage and Physical Mapping of Sex Region on LG23 of Nile Tilapia (Oreochromis niloticus). G3 Genes|Genomes|Genetics. 2012;2: 35–42. doi:10.1534/g3.111.001545

120. Liu X, Zhou L, Li W, Zhang L, Li M, Wang D. Production of fertile YY pseudofemales in Nile tilapia with LG23 as the sex chromosome. Aquaculture. 2024;587: 740870. doi:10.1016/j.aquaculture.2024.740870

121. Yamazaki W, Tan SL, Taketo T. Role of the X and Y Chromosomes in the Female Germ Cell Line Development in the Mouse (Mus musculus). Sexual Development. 2023;16: 355–364. doi:10.1159/000521151

122. Lam TJ, Nagahama Y, Chan K, Hoar WS. Overripe eggs and postovulatory corpora lutea in the threespine stickleback, Gasterosteus aculeatus L., form trachurus. Can J Zool. 1978;56: 2029–2036. doi:10.1139/z78-273

123. Roufidou C, Sebire M, Katsiadaki I, Mustafa A, Schmitz M, Mayer I, et al. Overripening of eggs and changes in reproductive hormones in the threespine stickleback, Gasterosteus aculeatus. Evol Ecol Res. 2016;17: 583–601.

124. Roufidou C, Borg B. Ovarian fluid in the three-spined stickleback : effects of egg overripening and sex steroid treatment. Journal of Fish Biology. 2019;94: 446–457. doi:10.1111/jfb.13915

125. Levy ER, Burgoyne PS. The fate of XO germ cells in the testes of XO/XY and XO/XY/XYY mouse mosaics: evidence for a spermatogenesis gene on the mouse Y chromosome. Cytogenet Cell Genet. 1986;42: 208–213. doi:10.1159/000132280

126. Mazeyrat S, Saut N, Grigoriev V, Mahadevaiah SK, Ojarikre OA, Rattigan Á, et al. A Y-encoded subunit of the translation initiation factor Eif2 is essential for mouse spermatogenesis. Nat Genet. 2001;29: 49–53. doi:10.1038/ng717

127. Touré A, Szot M, Mahadevaiah SK, Rattigan A, Ojarikre OA, Burgoyne PS. A new deletion of the mouse Y chromosome long arm associated with the loss of Ssty expression, abnormal sperm development and sterility. Genetics. 2004;166: 901–912.

128. Vernet N, Mahadevaiah SK, Yamauchi Y, Decarpentrie F, Mitchell MJ, Ward MA, et al. Mouse Y-Linked Zfy1 and Zfy2 Are Expressed during the Male-Specific Interphase between Meiosis I and Meiosis II and Promote the 2nd Meiotic Division. PLOS Genetics. 2014;10: e1004444. doi:10.1371/journal.pgen.1004444

129. Yamauchi Y, Riel JM, Stoytcheva Z, Ward MA. Two Y Genes Can Replace the Entire Y Chromosome for Assisted Reproduction in the Mouse. Science. 2014;343: 69–72. doi:10.1126/science.1242544

130. Shaw DE, Ross WD, Lambert AV, White MA. Single cell RNA-sequencing reveals no evidence for meiotic sex chromosome inactivation in the threespine stickleback fish. bioRxiv; 2024. p. 2024.11.26.625488. doi:10.1101/2024.11.26.625488

131. Largiadèr CR, Fries V, Bakker TCM. Genetic analysis of sneaking and egg-thievery in a natural population of the three-spined stickleback (Gasterosteus aculeatus L.). Heredity. 2001;86: 459–468. doi:10.1046/j.1365-2540.2001.00850.x

132. Mehlis M, Rahn AK, Bakker TCM. Sperm quality but not relatedness predicts sperm competition success in threespine sticklebacks (Gasterosteus aculeatus). BMC Evol Biol. 2015;15: 74. doi:10.1186/s12862-015-0353-x

133. Mehlis M, Hilke LK, Bakker TCM. Attractive males have faster sperm in three-spined sticklebacks Gasterosteus aculeatus. Current Zoology. 2013;59: 761–768. doi:10.1093/czoolo/59.6.761

134. Arnold AP, Chen X. What does the “four core genotypes” mouse model tell us about sex differences in the brain and other tissues? Frontiers in Neuroendocrinology. 2009;30: 1–9. doi:10.1016/j.yfrne.2008.11.001

135. Arnold AP. Four Core Genotypes and XY* mouse models: Update on impact on SABV research. Neuroscience & Biobehavioral Reviews. 2020;119: 1–8. doi:10.1016/j.neubiorev.2020.09.021

136. Vries GJD, Rissman EF, Simerly RB, Yang L-Y, Scordalakes EM, Auger CJ, et al. A Model System for Study of Sex Chromosome Effects on Sexually Dimorphic Neural and Behavioral Traits. J Neurosci. 2002;22: 9005–9014. doi:10.1523/JNEUROSCI.22-20-09005.2002

137. Gatewood JD, Wills A, Shetty S, Xu J, Arnold AP, Burgoyne PS, et al. Sex Chromosome Complement and Gonadal Sex Influence Aggressive and Parental Behaviors in Mice. J Neurosci. 2006;26: 2335–2342. doi:10.1523/JNEUROSCI.3743-05.2006

138. Suster ML, Abe G, Schouw A, Kawakami K. Transposon-mediated BAC transgenesis in zebrafish. Nat Protoc. 2011;6: 1998–2021. doi:10.1038/nprot.2011.416

139. Montague TG, Cruz JM, Gagnon JA, Church GM, Valen E. CHOPCHOP: a CRISPR/Cas9 and TALEN web tool for genome editing. Nucleic Acids Research. 2014;42: W401–W407. doi:10.1093/nar/gku410

140. Labun K, Montague TG, Gagnon JA, Thyme SB, Valen E. CHOPCHOP v2: a web tool for the next generation of CRISPR genome engineering. Nucleic Acids Research. 2016;44: W272–W276. doi:10.1093/nar/gkw398

141. Labun K, Montague TG, Krause M, Torres Cleuren YN, Tjeldnes H, Valen E. CHOPCHOP v3: expanding the CRISPR web toolbox beyond genome editing. Nucleic Acids Research. 2019;47: W171–W174. doi:10.1093/nar/gkz365

142. Subedi A, Macurak M, Gee ST, Monge E, Goll MG, Potter CJ, et al. Adoption of the Q transcriptional regulatory system for zebrafish transgenesis. Methods. 2014;66: 433–440. doi:10.1016/j.ymeth.2013.06.012

143. Kingsley DM, Zhu B, Osoegawa K, De Jong PJ, Schein J, Marra M, et al. New Genomic Tools for Molecular Studies of Evolutionary Change in Threespine Sticklebacks. Behaviour. 2004;141: 1331–1344.

144. Archambeault SL, Bärtschi LR, Merminod AD, Peichel CL. Adaptation via pleiotropy and linkage: Association mapping reveals a complex genetic architecture within the stickleback Eda locus. Evolution Letters. 2020;4: 282–301. doi:10.1002/evl3.175

145. Collins III JJ, Hou X, Romanova EV, Lambrus BG, Miller CM, Saberi A, et al. Genome-Wide Analyses Reveal a Role for Peptide Hormones in Planarian Germline Development. PLOS Biology. 2010;8: e1000509. doi:10.1371/journal.pbio.1000509

146. Square TA, Sundaram S, Mackey EJ, Miller CT. Distinct tooth regeneration systems deploy a conserved battery of genes. EvoDevo. 2021;12: 4. doi:10.1186/s13227-021-00172-3

147. Edgar RC. Muscle5: High-accuracy alignment ensembles enable unbiased assessments of sequence homology and phylogeny. Nat Commun. 2022;13: 6968. doi:10.1038/s41467-022-34630-w

148. Paradis E, Schliep K. ape 5.0: an environment for modern phylogenetics and evolutionary analyses in R. Bioinformatics. 2019;35: 526–528. doi:10.1093/bioinformatics/bty633

149. Mayor C, Brudno M, Schwartz JR, Poliakov A, Rubin EM, Frazer KA, et al. VISTA : visualizing global DNA sequence alignments of arbitrary length. Bioinformatics. 2000;16: 1046–1047. doi:10.1093/bioinformatics/16.11.1046

150. Frazer KA, Pachter L, Poliakov A, Rubin EM, Dubchak I. VISTA: computational tools for comparative genomics. Nucleic Acids Research. 2004;32: W273–W279. doi:10.1093/nar/gkh458

151. Brudno M, Do CB, Cooper GM, Kim MF, Davydov E, Program NCS, et al. LAGAN and Multi-LAGAN: Efficient Tools for Large-Scale Multiple Alignment of Genomic DNA. Genome Res. 2003;13: 721–731. doi:10.1101/gr.926603

152. Bolger AM, Lohse M, Usadel B. Trimmomatic: a flexible trimmer for Illumina sequence data. Bioinformatics. 2014;30: 2114–2120. doi:10.1093/bioinformatics/btu170

153. Zhang Y, Park C, Bennett C, Thornton M, Kim D. Rapid and accurate alignment of nucleotide conversion sequencing reads with HISAT-3N. Genome Res. 2021;31: 1290–1295. doi:10.1101/gr.275193.120

154. Putri GH, Anders S, Pyl PT, Pimanda JE, Zanini F. Analysing high-throughput sequencing data in Python with HTSeq 2.0. Bioinformatics. 2022;38: 2943–2945. doi:10.1093/bioinformatics/btac166

155. Love MI, Huber W, Anders S. Moderated estimation of fold change and dispersion for RNA-seq data with DESeq2. Genome Biology. 2014;15: 550. doi:10.1186/s13059-014-0550-8